Article

Benzothiazole and Chromone Derivatives as Potential ATR Kinase Inhibitors and Anticancer Agents

Mykhaylo Frasinyuk [1,†], Dimple Chhabria [2,†], Victor Kartsev [3,‡], Haritha Dilip [2,‡], Samvel N. Sirakanyan [4], Sivapriya Kirubakaran [2,*], Anthi Petrou [5], Athina Geronikaki [5,*] and Domenico Spinelli [6,*]

1   V.P. Kukhar Institute of Bioorganic Chemistry and Petrochemistry, National Academy of Science of Ukraine, 02094 Kiev, Ukraine; mykhaylo.frasinyuk@ukr.net
2   Discipline of Chemistry, Indian Institute of Technology Gandhinagar, Gandhinagar 382055, India; dimple.c@iitgn.ac.in (D.C.); d_haritha@iitgn.ac.in (H.D.)
3   InterBioScreen, 119019 Chernogolovka, Russia; vkartsev@ibscreen.chg.ru
4   Scientific Technological Center of Organic and Pharmaceutical Chemistry, National Academy of Science of the Republic of Armenia, Institute of Fine Organic Chemistry, Yerevan 0014, Armenia; shnnr@mail.ru
5   School of Pharmacy, Aristotle University of Thessaloniki, 54124 Thessaloniki, Greece; anthi.petrou.thessaloniki1@gmail.com
6   Dipartimento di Chimica "G. Ciamician", Alma Mater Studiorum-Università di Bologna, 40126 Bologna, Italy
*   Correspondence: priyak@iitgn.ac.in (S.K.); geronik@pharm.auth.gr (A.G.); domenico.spinelli@unibo.it (D.S.)
†   These authors contributed equally to this work.
‡   These authors contributed equally to this work.

Abstract: Despite extensive studies and the great variety of existing anticancer agents, cancer treatment remains an aggravating and challenging problem. Therefore, the development of novel anticancer drugs with a better therapeutic profile and fewer side effects to combat this persistent disease is still necessary. In this study, we report a novel series of benzothiazole and chromone derivatives that were synthesized and evaluated for their anticancer activity as an inhibitor of ATR kinase, a master regulator of the DDR pathway. The cell viability of a set of 25 compounds was performed using MTT assay in HCT116 and HeLa cell lines, involving 72 h incubation of the compounds at a final concentration of 10 μM. Cells incubated with compounds **2c**, **7h** and **7l** were found to show viability ≤50%, and were taken forward for dose–response studies. Among the tested compounds, three of them (**2c**, **7h** and **7l**) showed higher potency, with compound **7l** exhibiting the best IC$_{50}$ values in both the cell lines. Compounds **2c** and **7l** were found to be equally cytotoxic towards both the cell lines, namely, HCT116 and HeLa, while compound **7h** showed better cytotoxicity towards HeLa cell line. For these three compounds, an immunoblot assay was carried out in order to analyze the inhibition of phosphorylation of Chk1 at Ser 317 in HeLa and HCT116 cells. Compound **7h** showed inhibition of pChk1 at Ser 317 in HeLa cells at a concentration of 3.995 μM. Further analysis for Chk1 and pChk1 expression was carried out in Hela cells by treatment against all the three compounds at a range of concentrations of 2, 5 and 10 μM, wherein compound **7h** showed Chk1 inhibition at 2 and 5 μM, while pChk1 expression was observed for compound **7l** at a concentration of 5 μM. To support the results, the binding interactions of the compounds with the ATR kinase domain was studied through molecular docking, wherein compounds **2c**, **7h** and **7l** showed binding interactions similar to those of Torin2, a known mTOR/ATR inhibitor. Further studies on this set of molecules is in progress for their specificity towards the ATR pathway.

Keywords: benzothiazole; chromone; kinase inhibitor; anticancer

1. Introduction

Cancer remains one of the main leading causes of mortality all over the world. Despite extensive studies and the great variety of existing anticancer agents, cancer treatment remains an aggravating and challenging problem. Therefore, the development of novel

anticancer drugs with a better therapeutic profile and fewer side effects to combat this persistent disease is still necessary.

Cells are prone to a multitude of stress factors including endogenous and exogenous factors, such as reactive oxygen species, radiation, etc., which result in genomic instability through either a single strand or a double strand break in their DNA [1]. In order to cope with the stress, and to maintain genomic integrity as well as cell viability, cells develop DNA damage response (DDR) signaling pathways which regulate and repair the damage caused [2,3]. Targeting such crucial signaling pathways in cancer cells can prevent these cells from repairing their damaged single and/or double stranded DNA, hence promoting an efficient therapeutic strategy for cancer. Rad-3 related (ATR) and ataxia telangiectasia mutated (ATM) kinases from the phosphatidylinositol-3-kinase-related kinases (PIKK) family are two major signaling proteins which phosphorylate Ser/Thr residues of their downstream substrates Chk1 and CHk2, respectively [2–4]. The significant role of benzothiazoles as potential kinase inhibitors generates interest in exploring the biological activity of these compounds further in the area of kinases and thus, as potential candidates for cancer therapy [5].

Benzothiazole is a heterocyclic organic compound with a wide range of biological activities such as antimicrobial [6,7], anti-inflammatory [8,9], antioxidant [10,11], analgesic [8,12], anticancer [13–16], antiviral [17–20], anti-HIV [21,22], antidiabetic [23], anticonvulsant [24,25], antimalarial [26], antitubercular [27,28] and kinase inhibitor [29,30]. It should be mentioned that some FDA-approved drugs involve a benzothiazole carrier scaffold (Figure 1). They include quizartinib, a receptor tyrosine kinase inhibitor, flutemetamol, a diagnostic tool for Alzheimer disease, and riluzole, a drug for treatment of amyotrophic lateral sclerosis.
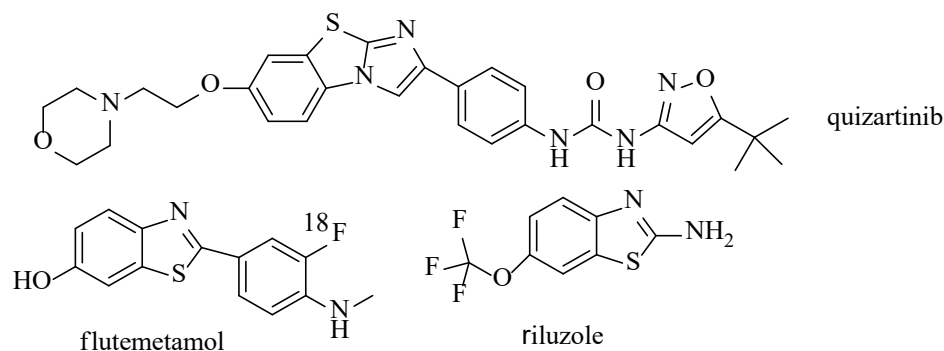

Figure 1. FDA-approved drugs.

On the other hand, chromone derivatives possess many different biological activities such as anticancer [31–33], antimicrobial [34], anti-inflammatory [35,36], antitubercular [37,38] and others activities [39–41], which have generated an interest in developing further this scaffold. The chromone scaffold is also present in some approved drugs such as flavoxate (Figure 2), a muscarinic antagonist and spasmolytic. This drug is used to treat urinary bladder spasms and is indicated for the symptomatic relief of conditions associated with lack of muscle control in the bladder, such as dysuria, urgency, and nocturia.
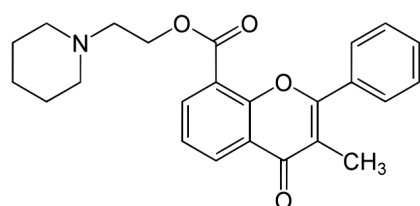

Figure 2. Flavoxate, FDA-approved drug.

Taking into account these facts, we designed and synthesized new derivatives incorporating two pharmacophores, benzothiazole and chromone, in the frame of one molecule using the hybridization approach [42]. Hence, in the present study, the synthesized hybrid molecules have been analyzed for their inhibitory potential against cancer cell viability, especially on the colon cancer and cervical cancer cell lines. Further, to identify their potential in inhibiting the DDR signaling pathway, the compounds have also been subjected to assays that specifically inhibit ATR expression in these cancer cells.

2. Results and Discussion

2.1. Chemistry

The general routes for the synthesis of the target 3-hetarylchromones include the synthesis of α-[benzo]thiazolyl acetophenones **1**, ring-closure reaction for synthesis of 3-(2[benzo])thiazolyl chromones **2–4**, modification of the substituent in position 2 of the chromone ring, and aminomethylation of 7-hydroxychromones. The starting ketones **1a–1f** were synthesized by Hoesch reaction of (un)substituted resorcinol with heteroaryl acetonitriles followed by subsequent acidic hydrolysis of intermediate ketone imines [43–45].

Subsequent reaction of ketones **1** with ethyl orthoformate, acetic anhydride or ethyl oxalyl chloride in pyridine afforded 3-heteroaryl chromones **2–4**.

Thus, refluxing of ketones **1a–1c** and **1e** with ethyl orthoformate in dry pyridine led to the formation of 2-unsubstituted chromones **2a–2c** and **2e**. Ring-closure reaction of ketones **1a** or **1c** with excess of acetic anhydride in dry pyridine with subsequent saponification led to 2-methylchromones **3a** and **3c**. Reaction of ketones **1a,b,d** with ethyl oxalyl chloride in dry pyridine at room temperature afforded 2-ethoxycarbonyl-3-benzotiazolylchromones **4a**, **4b**, and **4c**. Saponification of ester **4c** in EtOH gave carboxylic acid **4d**.

The reaction of 2-unsubstituted chromones **2a** or **2e** [46] with hydroxylamine in pyridine afforded 2-aminochromones **5a** or **5b** as a result of subsequent ring-opening and ring-closure reactions. This unusual behavior of chromones **2a** or **2e** toward hydroxylamine can be explained by the strong electron-withdrawing effect of the aza-heterocyclic moiety in position 3 of the chromone ring. The bearing of ω-carboxyalkyl group 3-hetarylchromones **6a–6d** and related 3-aryl-4-(2-benzothiazolyl)pyrazole **6e** were synthesized as we have earlier reported [47] (Scheme 1).

The aminomethylation of chromones with electron-withdrawing substituent in position 3 is possible by applying corresponding aminals [48]. Thus, the reaction of chromones **2–5** with various aminals led to regiospecific formation of 8-aminomethylchromones **7a–7m** (Scheme 2) which was confirmed by the disappearance in ^{1}H-NMR spectra of the upfield (for 6-alkyl substituted chromones **2–4**) peak or presence of H-6 doublet at 6.84–6.98 ppm with ^3J 8.3–8.8 Hz. The best yields were achieved using 1,4-dioxane as solvent.

Thus, in chromone Mannich bases **7** the singlet peak (except for compounds **7c**, **7j–7l**) of methylene group at 4.02–4.20 ppm was present as well as the secondary amine moiety. In the instance of piperidine and piperazine derivatives, in ^{1}H-NMR spectra signals of cyclic amine protons usually appear as wide non-resolved multiplets. In the case of chromones **7j–7l** with 1,3,3-trimethyl-6-azabicyclo [3.2.1]octane moiety, we observed two doublets of diastereotopic 8-CH$_2$ group at 4.00–4.05 ppm and 4.28–4.32 ppm with heminal J 14.3–14.5 Hz. In ^{1}H-NMR peaks of 8-CH$_2$ group, we observed two multiplets at 3.90 and 4.33 ppm due to difficult conversion of the piperidine ring and/or the presence of stereocenter.

Isomeric Mannich bases of 7-hydroxy-3-arylcoumarins were synthesized in similar conditions applying 3-(2-benzothiazolyl)-7-hydroxycoumarin (**8**) [49] and substituted 3-(2-thiazolyl)coumarins **9a,b** [50] (Scheme 3).
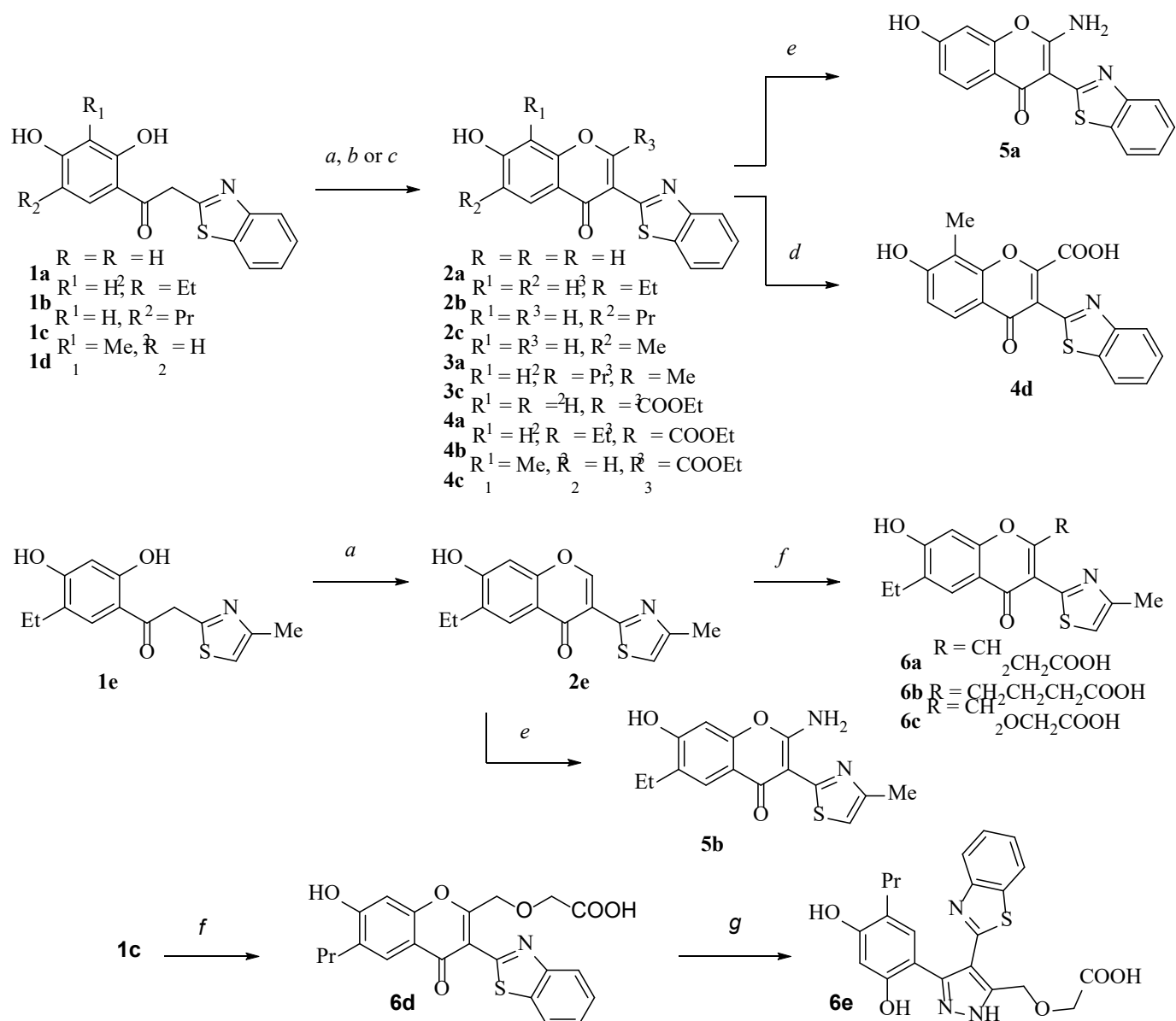
Scheme 1. Synthesis of the key intermediates 3-hetaryl chromones **2–5** and target compounds (**2c, 4a,b**, and **5a**). Reagents and conditions: (a) HC(OEt)$_3$, pyridine, 120 °C, 4–6 h; (b) *i* (CH$_3$CO)$_2$O, pyridine, r.t. 24–48 h; *ii* NaOH, EtOH, reflux, 1 min; (c) EtOOCCOCl, pyridine, r.t., 24–48 h; (d) LiOH, THF, r. t. 72 h; (e) NH$_2$OH·HCl, pyridine, reflux, 6–8 h; (f) succinic, glutaric or diglycolic anhydride, pyridine, r.t. 72 h; (g) hydrazine, EtOH, reflux, 4 h.

The synthesis of 8-aminomethyl derivatives was confirmed by splitting of H-5 and H-6 of coumarin core with ^3J 8.6–8.7 Hz. Similar to chromone **7** derivatives, the signal of 8-CH$_2$ group was found as a singlet at 3.99–4.23 ppm for diethanolamine, piperidine or piperazine derivatives. In the case of compound **11f**, the signals of 8-CH$_2$ group were found as two doublets at 4.07 and 4.37 ppm with ^2J 14.6 Hz.

Scheme 2. Synthesis of compounds **7a–7m**.
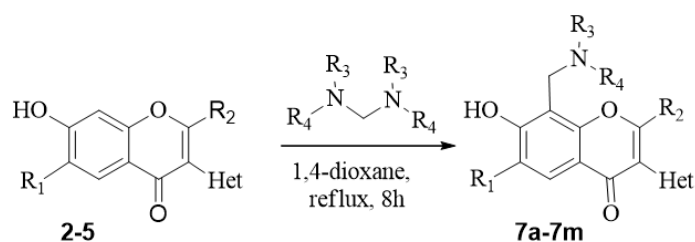
	R₁	R₂	NR₃R₄	Het
7a	H	Me	NMe₂	benzothiazol-2-yl
7b	H	Me	pyrrolidin-1-yl	benzothiazol-2-yl
7c	H	Me	2-methylpiperidin-1-yl	benzothiazol-2-yl
7d	H	Me	3-methylpiperidin-1-yl	benzothiazol-2-yl
7e	H	Me	4-methylpiperidin-1-yl	benzothiazol-2-yl
7f	H	Me	morpholin-4-yl	benzothiazol-2-yl
7g	Pr	Me	4-methylpiperazin-1-yl	benzothiazol-2-yl
7h	H	NH₂	4-methylpiperazin-1-yl	benzothiazol-2-yl
7i	Pr	Me	(4-(2-hydroxyethyl)piperazin-1-yl	benzothiazol-2-yl
7j	Et	H	1,3,3-trimethyl-6-azabicyclo [3.2.1]oct-6-yl	benzothiazol-2-yl
7k	H	Me	1,3,3-trimethyl-6-azabicyclo [3.2.1]oct-6-yl	benzothiazol-2-yl
7l	Et	CO₂Et	1,3,3-trimethyl-6-azabicyclo [3.2.1]oct-6-yl	benzothiazol-2-yl
7m	Et	NH₂	Piperidin-1-yl	4-methylthiazol-2-yl

Scheme 2. Synthesis of compounds **7a–7m**.
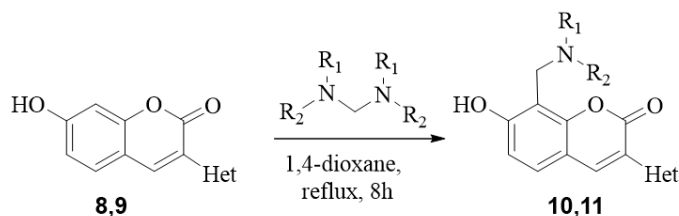
	NR₁R₂	Het
10a	N(CH₂CH₂OH)₂	benzothiazol-2-yl
10b	3,3-dimethylpiperidin-1-yl	benzothiazol-2-yl
10c	(4-(2-hydroxyethyl)piperazin-1-yl	benzothiazol-2-yl
11a	(4-(2-hydroxyethyl)piperazin-1-yl	4-methylthiazol-2-yl
11b	(4-(2-hydroxyethyl)piperazin-1-yl	4-(4-bromophenyl)thiazol-2-yl
11c	2-methylpiperidin-1-yl	4-(4-bromophenyl)thiazol-2-yl
11d	3-methylpiperidin-1-yl	4-(4-bromophenyl)thiazol-2-yl
11e	4-methylpiperidin-1-yl	4-(4-bromophenyl)thiazol-2-yl
11f	1,3,3-trimethyl-6-azabicyclo [3.2.1]oct-6-yl	4-methylthiazol-2-yl

Scheme 3. Synthesis of coumarin Mannich bases **10–11**.

2.2. Biological Evaluation

2.2.1. Cell Viability Studies—Initial Screening

In order to determine the effect of the compounds on cell viability, the studies were carried out using MTT assay in HCT116 and HeLa cell lines. Initial screening of the compounds was carried out at a final concentration of 10 μM. The cell viability was reduced by ≤50% in the presence of three compounds, namely **2c**, **7h** and **7l**, hence showing cell

toxicity in both cell lines at a final concentration of 10 μM. Figure 3 represents the initial screening results for HCT116 cells after 72 h incubation.
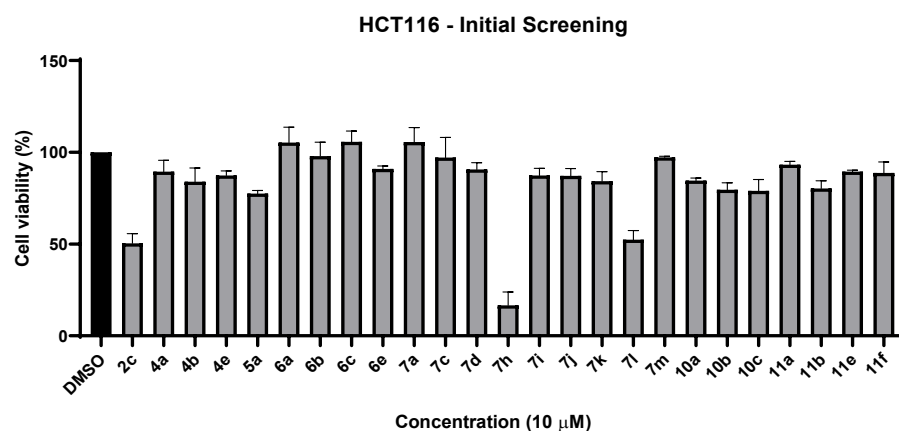

Figure 3. Initial screening results for HCT116 cells after 72 h incubation.

Similarly, Figure 4 represents the initial screening results for HeLa cells after 72 h incubation.
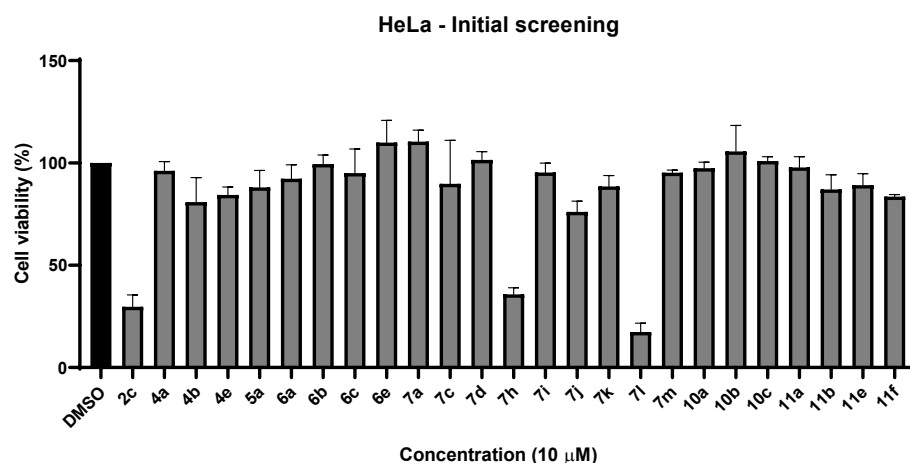

Figure 4. Initial screening results for HeLa cells after 72 h incubation.

Compounds **2c**, **7h** and **7l** showed a significant reduction in cell viability for both the cervical cancer and colon cancer cell lines, suggesting that these compounds could be potent anticancer agents, especially for these two types of cancer. In order to identify the minimum concentration of these compounds required to reduce the cell viability of these cell lines by 50% or more, these compounds were further analyzed for their cytotoxicity effects using dose-response studies. The dose-response studies would be performed under similar conditions as those for the initial screening, for a concentration range of the potent compounds, so as to identify the half maximal inhibitory concentration (IC_{50}) of each compound required to cause cell toxicity.
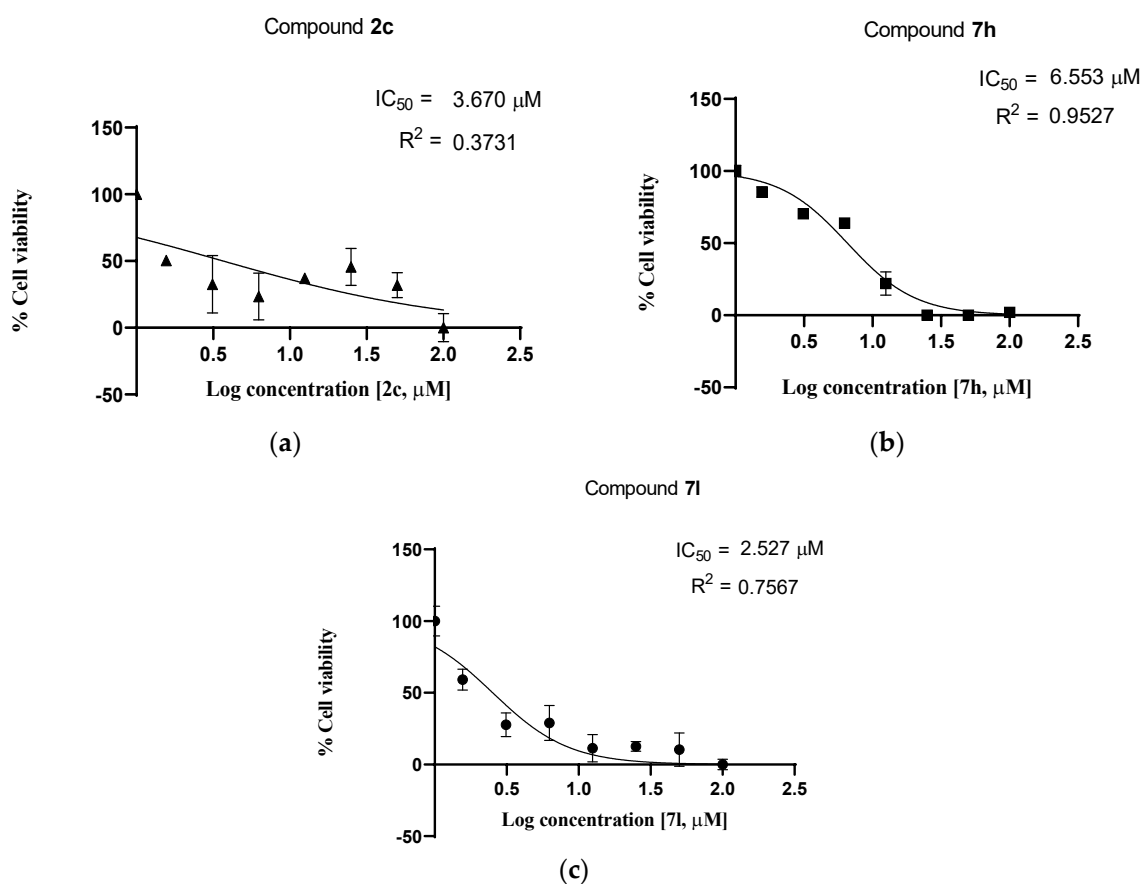
2.2.2. Cell Viability Studies—Dose Response

The dose–response studies were conducted using the MTT assay for **2c**, **7h** and **7l**, for a dose range of 0–100 μM similar to the initial screening protocol. Further, the absorbance was measured at 570 nm using the PerkinElmer EnVision Multilabel Reader and the IC_{50} values calculated for all the three compounds (Table 1).

Table 1. IC$_{50}$ values of compounds in HCT116 and HeLa.

| Sl. No. | Compound | IC$_{50}$ Value (µM) | |
		HCT116	HeLa
1	**2c**	3.670	2.642
2	**7h**	6.553	3.995
3	**7l**	2.527	2.659

Figure 5 represents the dose–response curves for the compounds **2c**, **7h** and **7l** in HCT116 cells after 72 h incubation.

Compound **2c**

IC$_{50}$ = 3.670 µM

R^2 = 0.3731

(**a**)

Compound **7h**

IC$_{50}$ = 6.553 µM

R^2 = 0.9527

(**b**)

Compound **7l**

IC$_{50}$ = 2.527 µM

R^2 = 0.7567

(**c**)

Figure 5. Dose response curves for the compounds in HCT116 cells after 72 h incubation.

Similarly, Figure 6 represents the dose–response curves for the compounds **2c**, **7h** and **7l** in HCT116 cells after 72 h incubation.

Compounds **2c** and **7h** showed IC$_{50}$ values of 3.670 µM and 6.553 µM against HCT116 cell lines, while **7l** showed an IC$_{50}$ value of 2.527 µM. However, all three compounds were equally potent against the HeLa cell line with IC$_{50}$ values of 2.642 µM, 3.995 µM and 2.659 µM, respectively. Further, to analyze the effect of these compounds specifically on the DDR signaling pathway, an essential pathway for cancer cell survival, the compounds were subjected to cell-based assays that would determine the inhibition of these pathways.
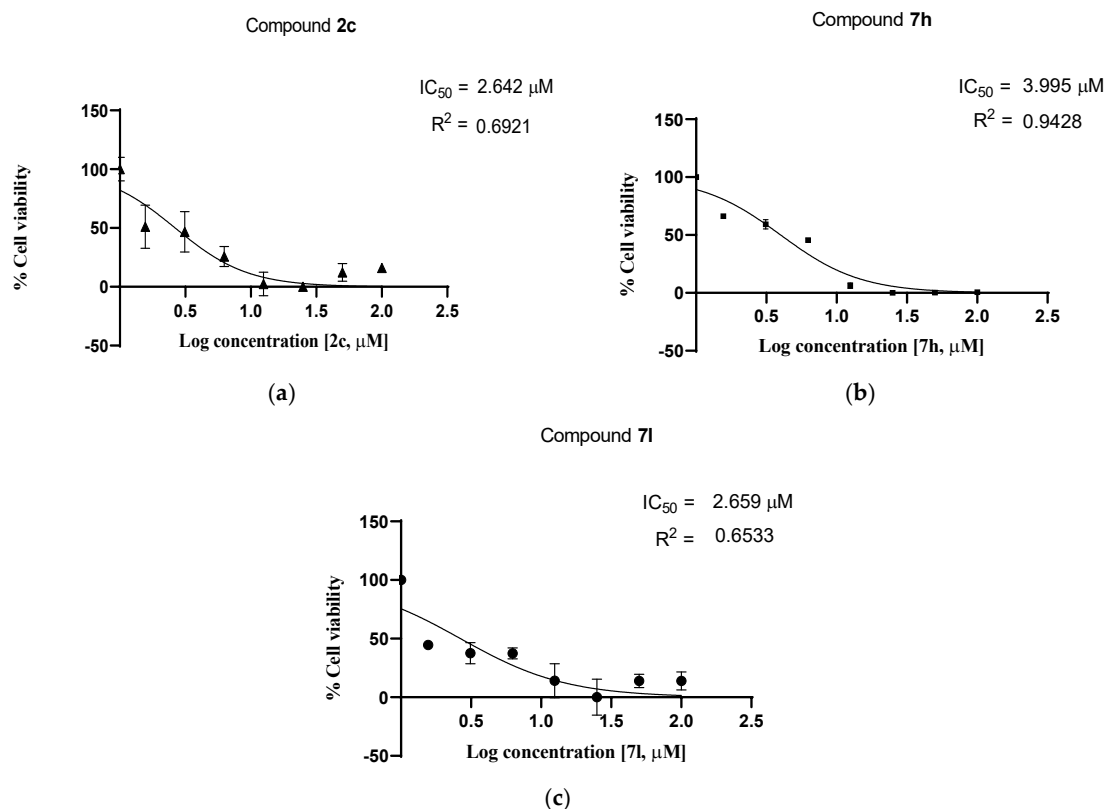
Compound **2c**

IC$_{50}$ = 2.642 µM

R^2 = 0.6921

Compound **7h**

IC$_{50}$ = 3.995 µM

R^2 = 0.9428

(**a**)

(**b**)

Compound **7l**

IC$_{50}$ = 2.659 µM

R^2 = 0.6533

(**c**)

Figure 6. Dose–response curves for the compounds in HeLa cells after 72 h incubation.

2.2.3. Immunoblot Assay

The effect of the synthesized compounds to inhibit the cancer cell's DNA damage response (DDR) signalling pathway, a common pathway preferred by cancer cells to ensure genomic integrity, as well as cell viability [51], was analyzed by carrying out an immunoblot assay for one of the major kinases involved in the regulation of the pathway. Ataxia telangiectasia mutated and Rad-3 related (ATR) kinase, a member of the the PIKK (phosphatidylinositol-3-kinase-related kinases) family, are involved in the phosphorylation of Ser/Thr residues of its downstream substrate Chk1. The inhibition of Chk1 phosphorylation has been proved to be a clear indication of the inhibition of ATR signalling. Hence, the immunoblot assay helps in the determination of the inhibitory potential of the synthesized compounds against ATR kinase in the DDR pathway.

The analysis of inhibition of phosphorylation of Chk1 at Ser 317 in HeLa and HCT116 cells was carried out by immunoblotting using anti-pChk1 Ser 317 (rabbit) primary antibody and anti-rabbit IgG HRP-linked secondary antibody. Of the three compounds tested, compound **7h** showed inhibition of ATR signaling which was observed by checking the status of ChK1 in HeLa cells (Figure 7). However, the results for HCT116 do not show significant inhibition of ATR signaling in the cases of compounds **7h** and **2c**, while **7l** showed inhibition with respect to the control.

Further, to analyze the effect of the concentration of the compounds on the expression of Chk1 and pChk1 at Ser 317 in HeLa cells, immunoblotting assay using ChK1 mouse monoclonal antibody, and anti-pChk1 Ser 317 (rabbit) primary antibody were carried out. Anti-mouse IgG HRP-linked antibody and anti-rabbit IgG HRP-linked secondary antibody were used as secondary antibodies, respectively. The inhibition of Chk1 was observed at 2 µM and 5 µM concentrations of compound **7h**. In the cases of compounds **2c** and **7l**, the ChK1 and pChK1 expression in the control lanes did not provide a clear insight into the inhibition of ATR signaling (Figure 8).
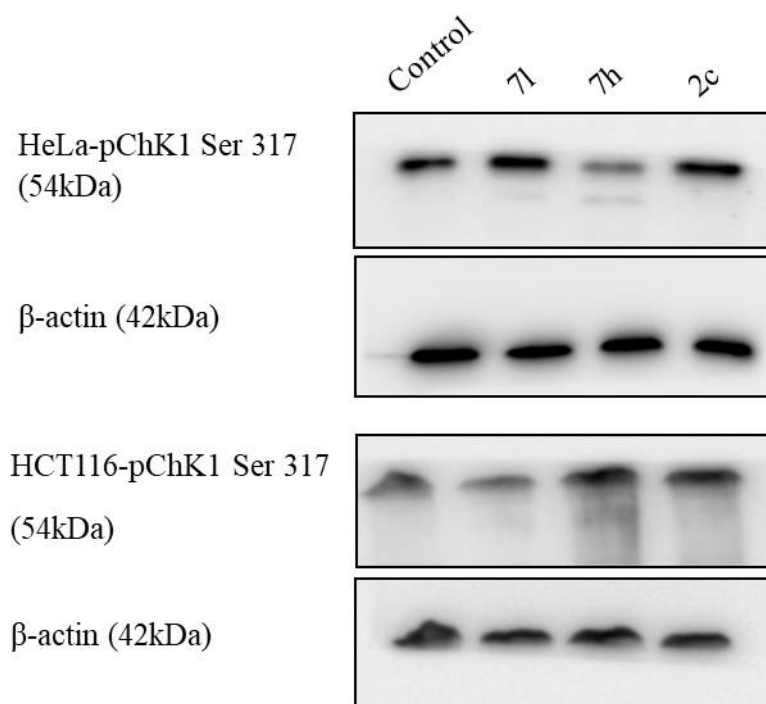
Figure 7. Inhibition of Chk1 at Ser 317 in HeLa and HCT116 cells analyzed by immunoblot assay.
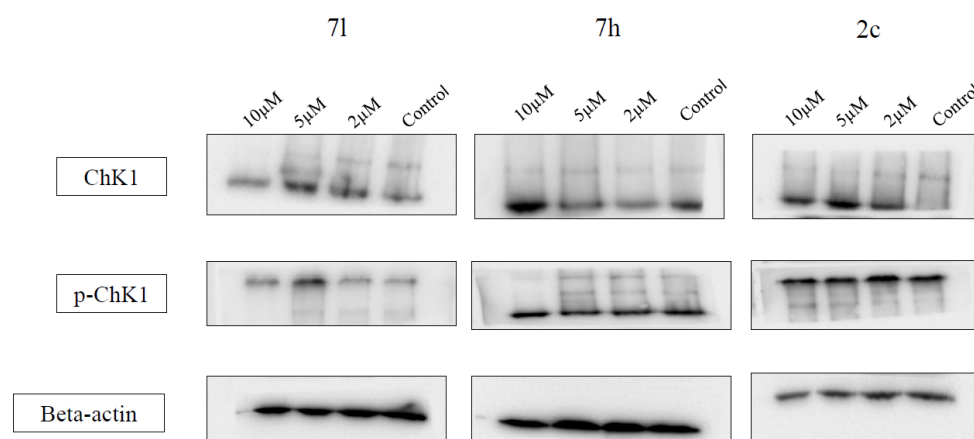

Figure 8. Expression of Chk1 and pChk1 at Ser 317 in cells analyzed by immunoblot assay with respect to treatment against compounds **7l**, **7h** and **2c**.

2.3. Molecular Docking

The use of molecular docking as a successful computational tool in drug discovery, to model and visualize the interactions between small molecules and their specific targets, has been prevalent since the 1980s. The conformations and binding interactions corresponding to the behavior of the small molecules at the binding site of the drug target have also been an essential factor in identifying the mechanism of enzyme inhibition, which further enhance the drug development processes [52].

Molecular docking resulted in an in-depth analysis of the major binding interactions between the compounds with the ATR kinase domain. Compound **2c** showed the same GScore and DockScore of −5.5 kcal/mol, followed by a GScore and DockScore of −5.2 kcal/mol and −5.1 kcal/mol for Torin2. Compound **7l** showed the GScore and DockScore of −5.2 kcal/mol and −4.8 kcal/mol. This was followed by compound **7h** with a GScore and DockScore of −4.3 kcal/mol and −3.4 kcal/mol (Table 2).

Table 2. Molecular docking results for Torin2 and compounds **2c**, **7h** and **7l**.

Sl. No.	Interaction	Point Interaction	Donor Atom	Acceptor Atom	Type of Interaction	Bond Distance (Å)	Binding Energy (Dock Score) (kcal/mol)
1.	**2c**	**2c** OH–Val 88	**2c**: O	Val 88	Hydrogen bond	1.72	−5.5
		2c aromatic ring–Trp 87	**2c**: aromatic ring	Trp 87	π-π stacking	3.37, 3.81, 3.87	
		2c benzothiazole–Lys 16	**2c**: benzothiazole	Lys 16	π-Cation interaction	5.15, 5.37	
2.	**Torin2**	Lys 100–Torin2 O	Lys 100	Torin2: O	Hydrogen bond	1.80	−5.1
		Torin2 NH₂–Val 88	Torin2: N	Val 88	Hydrogen bond	2.31	
		Lys 16–Torin2 N	Lys 16	Torin2: N	Hydrogen bond	2.01	
		Torin2 pyridine–Trp 87	Torin2: pyridine	Trp 87	π-π stacking	3.47, 3.77	
3.	**7h**	**7h** OH–Asn 89	**7h**: O	Asn 89	Hydrogen bond	1.90	−3.4
		7h NH–Thr 91	**7h**: N	Thr 91	Hydrogen bond	1.93	
		7h benzothiazole–Trp 87	**2c**: benzothiazole	Trp 87	π-π stacking	4.00	
4.	**7l**	Lys 16–**7l** O	Lys 16	**7l**: O	Hydrogen bond	1.94	−4.8
		7l benzothiazole–Trp 87	**7l**: benzothiazole	Trp 87	π-π stacking	5.02	
		Lys 16–**7l** benzothiazole	Lys 16	**7l**: benzothiazole	π-Cation interaction	5.01	
		Lys 100–**7l** O	Lys 100	**7l**: O	Salt Bridge	2.80	

Two-dimensional ligand interaction diagrams show the major binding interactions between the compounds and the binding site of the ATR kinase domain. Torin2, the standard ligand had hydrogen bonding and π-π stacking interactions as the major interactions at the binding site. Compound **2c** had the highest docking score of −5.5 kcal/mol, wherein hydrogen bonding, π-π stacking and π-cation interactions played the major role. Compound **7h** had similar interactions in comparison to Torin2, with a lowest docking score of −3.4 kcal/mol. However, unlike all the ligands in the molecular docking study, compound **7l** had the highest number of diverse interactions at the binding site, including hydrogen bonding, π-π stacking, π-cation interactions and salt bridge formation. The ligand interaction diagrams for the binding interactions of compounds **2c**, **7h** and **7l** along with Torin2 are shown in Figure 9.
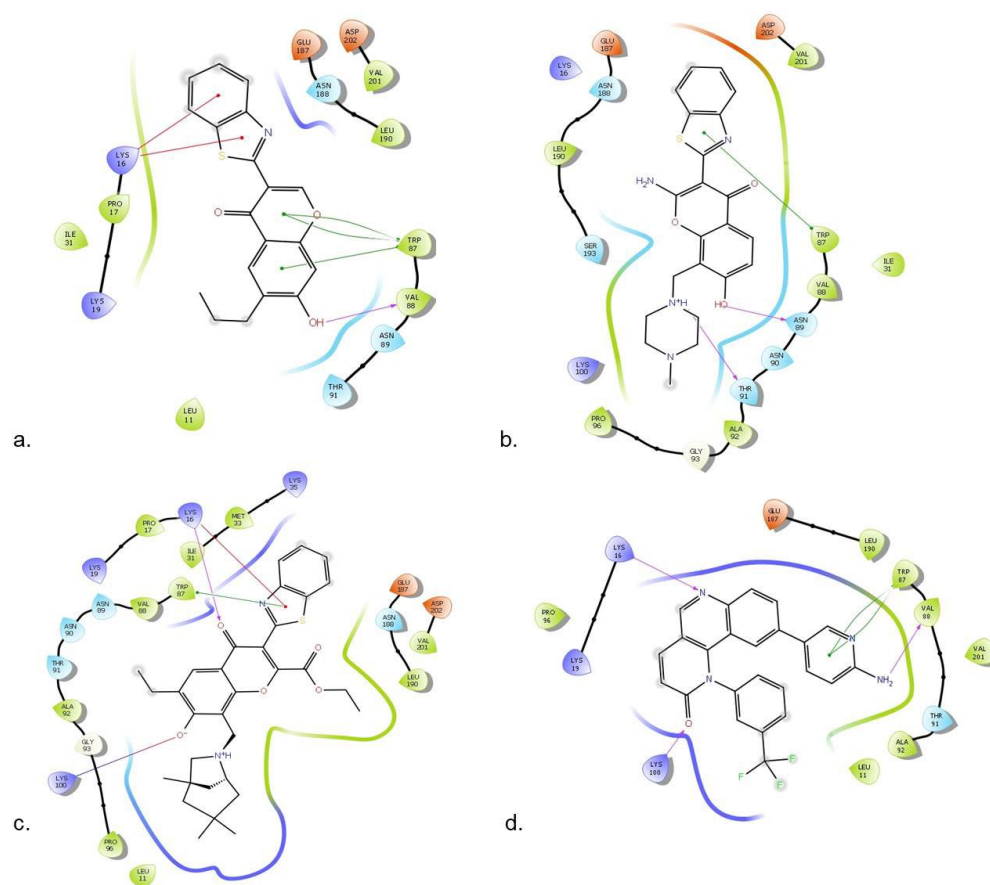

Figure 9. Ligand interaction diagrams for the compounds (**a**) **2c**, (**b**) **7h**, (**c**) **7l** and (**d**) Torin2.

The three-dimensional view of the ligand conformations in the binding site is crucial to visualize the interactions determined through ligand interaction diagrams. The binding poses of the compounds, in comparison to the standard ligand helps in deciphering the nature of binding of these compounds at the binding site. The 3D diagrams indicating the binding poses of the compounds **2c** (pink), **7h** (yellow), **7l** (orange) and Torin2 (green) are depicted in Figure 10.
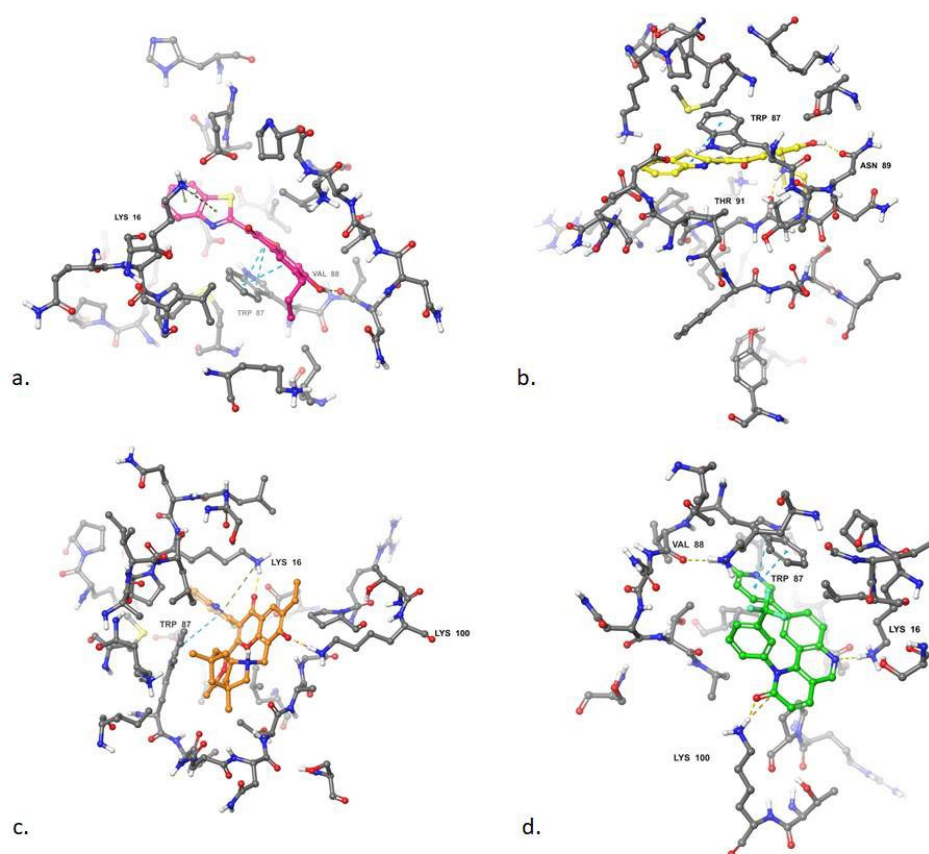
Figure 10. Binding pose for the compounds (**a**) 2c, (**b**) 7h, (**c**) 7l and (**d**) Torin2 at the binding site.

3. Materials and Methods

3.1. General Information

^{1}H and ^{13}C spectra were recorded on Varian 500 (500/125 MHz) or Varian 400 (400/100 MHz) and/or Varian VXR300 spectrometers in CDCl$_3$ [residual CHCl$_3$ (δ_H = 7.26 ppm) or CDCl$_3$ (δ_C = 77.16 ppm) as internal standard] or DMSO-d_6 [residual SO(CD$_3$)(CD$_2$H) (δ_H = 2.50 ppm) or SO(CD$_3$)$_2$ (δ_C = 39.52 ppm) as internal standard]. Melting points were determined in open capillary tubes using Buchi B-535 apparatus (Buchi Labortechnik AG, Flawil, Switzerland) and were uncorrected. Mass spectra were obtained using an Agilent 1100 spectrometer (Agilent Technologies, Waldbronn, Germany) using APCI (atmospheric-pressure chemical ionization). All spectra are available in Supplementary Materials.

Colon cancer cell line HCT116 and human cervical cancer cell line HeLa were furnished by National Centre for Cell Science (NCCS), Pune, India, DMEM from LONZA, Fetal bovine serum, pen-strap, and trypsin-EDTA from Invitrogen corporation (Carlsbad, CA, USA), MTT [3-(4,5-Dimethyl-2-thiazolyl)-2,5-diphenyl tetrazolium bromide] dye from HIMEDIA (Mumbai, India), and transparent 96-well plates from TARSON (Tarsons Products Pvt. Ltd., Mumbai, India).

Sodium dodecyl sulphate (SDS), tetramethylenediamine (TEMED), ammonium persulphate (APS), bromophenol blue and beta-mercaptoethanol were purchased from HIMEDIA (Mumbai, India), Tween-20 and Bovine serum albumin (BSA) from Sigma-Aldrich (Darmstadt, Germany), complete-EDTA free protease inhibitor tablets from Roche (Basel, Switzerland), immunoblot PVDF Western blotting membrane and Clarity ECL Western blotting substrate from Bio-Rad laboratories (Hercules, CA, USA), ChK1- phosphor Ser 317 (Cat. 12302S), ChK1 Mouse (Cat. 2360S) monoclonal antibody, Anti-mouse IgG HRP-linked antibody (Cat. 7076P2) and Anti-rabbit IgG HRP- linked secondary antibody (Cat. 7074) from Cell Signaling Technology (Danvers, MA, USA), and mouse anti-human Beta-actin (Cat. SC47778) from Santa Cruz Biotechnology (Dallas, TX, USA).

3.2. Chemistry

Compounds **1a** [43], **1b** [45], **1c** [44], **1e** [46], **2a** [43], **2b** [45], **2c** [44], **2e** [46], **3c** [44], **6a–6d** [47], **8** [48], and **9a,b** [49] were synthesized by procedures reported earlier.

2-(1,3-Benzothiazol-2-yl)-1-(2,4-dihydroxy-3-methylphenyl)ethanone (**1d**) was synthesized according to the literature procedure [44]. Yield 53%, m.p. 255–256 °C. LC-MS: m/z 300.0 [M + H]$^+$. ^{1}H-NMR (400 MHz, DMSO-d_6): δ ppm 14.52 (s, 1H), 12.65 (s, 1H), 9.96 (s, 1H), 7.76 (d, J = 7.7 Hz, 1H), 7.48 (d, J = 8.7 Hz, 1H), 7.39–7.30 (m, 2H), 7.21–7.11 (m, 1H), 6.69 (s, 1H), 6.43 (d, J = 8.6 Hz, 1H), 2.01 (s, 3H). ^{13}C-NMR (125 MHz, DMSO-d_6): δ ppm 186.0, 162.4, 161.9, 159.9, 138.8, 126.8, 126.7, 125.7, 122.5, 122.3, 112.1, 111.6, 110.4, 106.3, 85.9, 7.9. Elemental analysis for $C_{16}H_{13}NO_3S$; Calc.: C, 64.20; H, 4.38; N, 4.68%. Found: C, 64.22; H, 4.35; N, 4.70%.

3-(1,3-Benzothiazol-2-yl)-7-hydroxy-2-methyl-4H-chromen-4-one (**3a**) was synthesized according to the literature procedure [45]. Yield 78%, m.p. 292–293 °C. LC-MS: m/z 310.1 [M + H]$^+$. ^{1}H-NMR (400 MHz, DMSO-d_6): δ ppm 10.94 (s, 1H), 8.08 (d, J = 7.9 Hz, 1H), 8.04–7.93 (m, 2H), 7.53–7.45 (m, 1H), 7.44–7.37 (m, 1H), 6.95 (d, J = 8.7 Hz, 1H), 6.85 (s, 1H), 2.95 (s, 3H). ^{13}C-NMR (125 MHz, DMSO-d_6): δ ppm 173.7, 168.9, 163.1, 159.9, 156.4, 150.9, 135.0, 127.1, 125.8, 124.8, 122.3, 121.4, 115.6, 114.5, 114.4, 102.0, 21.7. Elemental analysis for $C_{17}H_{13}NO_3S$; Calc.: C, 66.01; H, 3.58; N, 4.53%. Found: C, 66.05; H, 3.60; N, 4.56%.

3.2.1. General Procedure for the Synthesis of 2-Ethoxycarbonyl Chromones **4a–4c**

To a solution of the corresponding starting compounds **1a,b,d** (5 mmol) in dry pyridine (10 mL) ethyl oxalyl chloride (15 mmol) was added dropwise under cooling. The reaction mixture was stirred for 24–48 h at room temperature and poured into 200 mL of 1N HCl. The formed precipitate was filtered off, dried, and re-crystallized from EtOH to furnish the desired products **4a–4c**.

Ethyl 3-(1,3-benzothiazol-2-yl)-7-hydroxy-4-oxo-4H-chromene-2-carboxylate (**4a**). Yield 67%, m.p. 223–224 °C, yellow crystals. LC-MS: m/z 368.0 [M + H]$^+$. ^{1}H-NMR (400 MHz, DMSO-d_6): δ ppm 11.23 (s, 1H), 8.17 (d, J = 7.9 Hz, 1H), 8.07 (d, J = 8.7 Hz, 1H), 7.98 (d, J = 8.1 Hz, 1H), 7.57–7.51 (m, 1H), 7.46 (t, J = 7.4 Hz, 1H), 7.06 (d, J = 8.8 Hz, 1H), 7.01 (s, 1H), 4.45 (q, J = 7.0 Hz, 2H), 1.24 (t, J = 7.0 Hz, 3H). ^{13}C-NMR (125 MHz, DMSO-d_6): δ ppm 173.5, 164.1, 161.1, 156.8, 156.6, 154.5, 150.8, 135.6, 127.4, 126.5, 125.4, 122.4, 122.1, 116.7, 115.1, 113.8, 102.5, 63.0, 13.6. Elemental analysis for $C_{19}H_{13}NO_5S$; Calc.: C, 62.12; H, 3.57; N, 3.81%. Found: C, 62.09; H, 3.60; N, 3.79%.

Ethyl 3-(1,3-benzothiazol-2-yl)-6-ethyl-7-hydroxy-4-oxo-4H-chromene-2-carboxylate (**4b**). Yield 74%, m.p. 192–193 °C, colorless. LC-MS: m/z 396.0 [M + H]$^+$. ^{1}H-NMR (500 MHz, DMSO-d_6): δ ppm 11.30 (s, 1H), 8.19 (d, J = 7.9 Hz, 1H), 7.98 (d, J = 8.1 Hz, 1H), 7.92 (s, 1H), 7.59–7.52 (m, 1H), 7.50–7.44 (m, 1H), 7.01 (s, 1H), 4.45 (q, J = 7.1 Hz, 2H), 2.67 (q, J = 7.4 Hz, 2H), 1.23 (t, J = 7.1 Hz, 3H), 1.21 (t, J = 7.4 Hz, 3H). ^{13}C-NMR (125 MHz, DMSO-d_6): δ ppm 173.3, 162.1, 161.2, 156.9, 154.9, 154.3, 150.8, 135.5, 131.9, 126.5, 125.4, 124.9, 122.4, 122.1, 114.8, 113.7, 101.7, 62.9, 22.4, 13.6, 13.5. Elemental analysis for $C_{21}H_{17}NO_5S$; Calc.: C, 63.79; H, 4.53; N, 3.54%. Found: C, 63.77; H, 4.49; N, 3.57%.

Ethyl 3-(1,3-benzothiazol-2-yl)-7-hydroxy-8-methyl-4-oxo-4H-chromene-2-carboxylate (**4c**). Yield 69%, m.p. 265–266 °C. LC-MS: m/z 382.0 [M + H]$^+$. ^{1}H-NMR (400 MHz, DMSO-d_6): δ ppm 11.07 (s, 1H), 8.16 (d, J = 7.7 Hz, 1H), 7.98 (d, J = 8.0 Hz, 1H), 7.93 (d, J = 8.7 Hz, 1H), 7.58–7.50 (m, 1H), 7.49–7.41 (m, 1H), 7.11 (d, J = 8.7 Hz, 1H), 4.47 (q, J = 7.0 Hz, 2H), 2.24 (s, 3H), 1.23 (t, J = 7.1 Hz, 3H). ^{13}C-NMR (125 MHz, DMSO-d_6): δ ppm 173.9, 161.6, 161.2, 156.9, 154.5, 154.5, 150.8, 135.6, 126.4, 125.3, 124.0, 122.4, 122.0, 115.2, 115.1, 113.4, 111.5, 62.9, 13.6, 7.9. Elemental analysis for $C_{20}H_{15}NO_5S$; Calc.: C, 62.98; H, 3.96; N, 3.67%. Found: C, 62.94; H, 3.99; N, 3.63%.

3-(1,3-Benzothiazol-2-yl)-7-hydroxy-8-methyl-4-oxo-4H-chromene-2-carboxylic acid (**4d**). To a stirred solution of ester **4d** (1 mmol) in THF (10 mL), a solution of LiOH·2H$_2$O (2 mmol) in water (2 mL) was added at room temperature. After stirring for 24 h, reaction was quenched by 1N HCl (5 mL), formed precipitate was filtered off, dried, and re-crystallized from EtOH to furnish the desired products **4e** as yellow crystals. Yield 58%, m.p. 342–343 °C. LC-MS:

m/z 354.0 [M + H]$^+$. ^{1}H-NMR (400 MHz, DMSO-d_6): δ ppm 11.16 (s, 1H), 8.16 (d, J = 7.8 Hz, 1H), 7.98 (d, J = 8.0 Hz, 1H), 7.92 (d, J = 8.7 Hz, 1H), 7.62–7.50 (m, 1H), 7.50–7.41 (m, 1H), 7.17 (d, J = 8.7 Hz, 1H), 2.26 (s, 3H). ^{13}C-NMR (125 MHz, DMSO-d_6): δ ppm 174.2, 162.4, 161.6, 157.5, 156.0, 154.5, 151.2, 135.7, 126.2, 125.2, 123.9, 122.5, 122.0, 115.2, 115.1, 113.0, 111.5, 7.9. Elemental analysis for $C_{18}H_{11}NO_5S$; Calc.: C, 61.18; H, 3.14; N, 3.96%. Found: C, 61.21; H, 3.12 N, 3.98%.

3.2.2. General Procedure for the Synthesis of 2-Aminochromones 5a,b

A mixture of chromone **2a,e** (1 mmol) and hydroxylamine hydrochloride (2 mmol) in pyridine (5 mL) was refluxed for 6–8 h. The reaction mixture was cooled, and the formed precipitate was filtered off, dried, and re-crystallized from EtOH to furnish the desired products **5a,b**.

2-Amino-3-(1,3-benzothiazol-2-yl)-7-hydroxy-4H-chromen-4-one (**5a**). Yield 46%, m.p. 364–365, colorless. °C. LC-MS: m/z 311.0 [M + H]$^+$. ^{1}H-NMR (400 MHz, DMSO-d_6): δ ppm 10.86 (s, 1H), 10.68 (s, 1H), 9.46 (s, 1H), 8.02 (d, J = 7.7 Hz, 1H), 7.98–7.90 (m, 2H), 7.49–7.40 (m, 1H), 7.36–7.28 (m, 1H), 6.89 (d, J = 8.6 Hz, 1H), 6.77 (s, 1H). ^{13}C-NMR (125 MHz, DMSO-d_6): δ ppm 172.2, 163.7, 162.8, 162.1, 153.6, 149.9, 133.0, 127.0, 125.7, 123.7, 121.3, 120.6, 114.0, 113.4, 101.6, 92.0. Elemental analysis for $C_{16}H_{10}N_2O_3S$; Calc.: C, 61.93; H, 3.25; N, 9.03%. Found: C, 61.91; H, 3.22; N, 9.00%.

2-Amino-6-ethyl-7-hydroxy-3-(4-methyl-1,3-thiazol-2-yl)-4H-chromen-4-one (**5b**). Yield 74%, m.p. 290–291 °C. LC-MS: m/z 303.2 [M + H]$^+$. ^{1}H-NMR (400 MHz, DMSO-d_6): δ ppm 10.57 (s, 2H), 9.00 (s, 1H), 7.76 (s, 1H), 6.96 (s, 1H), 6.78 (s, 1H), 2.60 (q, J = 7.3 Hz, 2H), 2.39 (s, 3H), 1.17 (t, J = 7.4 Hz, 3H). ^{13}C-NMR (125 MHz, DMSO-d_6): δ ppm 171.6, 162.9, 161.1, 159.5, 151.6, 147.9, 128.6, 124.8, 113.2, 111.2, 100.9, 92.2, 22.3, 16.8, 13.8. Elemental analysis for $C_{15}H_{14}N_2O_3S$; Calc.: C, 59.59; H, 4.67; N, 9.27%. Found: C, 59.57; H, 4.65; N, 9.30%.

3.2.3. General Procedure for Synthesis of 8-Aminomethyl Derivatives 7

A stirring mixture of the corresponding chromone (1 mmol) and aminal [44] (1.2 mmol) in 1,4-dioxane (5 mL) was refluxed for 6–8 h. The reaction mixture was cooled, diluted with 10 mL of hexane. The formed precipitate was filtered off, dried, and re-crystallized from iPrOH-hexanes mixture to furnish the desired chromone Mannich bases **7**.

3-(1,3-Benzothiazol-2-yl)-8-[(dimethylamino)methyl]-7-hydroxy-2-methyl-4H-chromen-4-one (**7a**). Yield 71%, m.p. 224–225 °C, pale pink. LC-MS: m/z 367.2 [M + H]$^+$. ^{1}H-NMR (500 MHz, CDCl$_3$): δ ppm 8.13 (d, J = 8.8 Hz, 1H), 8.05 (d, J = 8.1 Hz, 1H), 7.98 (d, J = 7.7 Hz, 1H), 7.52–7.45 (m, 1H), 7.43–7.35 (m, 1H), 6.92 (d, J = 8.8 Hz, 1H), 4.02 (s, 2H), 3.04 (s, 3H), 2.46 (s, 6H). ^{13}C-NMR (125 MHz, CDCl$_3$): δ ppm 175.2, 167.9, 164.7, 160.5, 154.3, 151.8, 136.1, 126.9, 125.8, 124.9, 122.8, 121.4, 116.2, 115.7, 115.2, 107.3, 55.3, 44.7, 22.0. Elemental analysis for $C_{20}H_{18}N_2O_3S$; Calc.: C, 65.55; H, 4.95; N, 7.64%. Found: C, 65.57; H, 4.93; N, 7.66%.

3-(1,3-Benzothiazol-2-yl)-7-hydroxy-2-methyl-8-(pyrrolidin-1-ylmethyl)-4H-chromen-4-one (**7b**). Yield 67%, m.p. 214–217 °C, colorless. LC-MS: m/z 393.0 [M + H]$^+$. ^{1}H-NMR (300 MHz, CDCl$_3$): δ ppm 11.47 (s, 1H), 8.12 (d, J = 8.8 Hz, 1H), 8.07–8.01 (m, 1H), 8.00–7.94 (m, 1H), 7.51–7.43 (m, 1H), 7.43–7.35 (m, 1H), 6.90 (d, J = 8.8 Hz, 1H), 4.19 (s, 2H), 3.03 (s, 3H), 2.91–2.66 (m, 4H), 2.03–1.83 (m, 4H). ^{13}C-NMR (125 MHz, CDCl$_3$): δ ppm 175.2, 167.9, 164.9, 160.6, 154.0, 151.8, 136.1, 126.7, 125.7, 124.8, 122.8, 121.4, 116.2, 115.7, 115.1, 107.8, 53.9, 51.4, 23.9, 22.0. Elemental analysis for $C_{22}H_{20}N_2O_3S$; Calc.: C, 67.33; H, 5.14; N, 7.14%. Found: C, 67.36; H, 5.12; N, 7.17%.

3-(1,3-Benzothiazol-2-yl)-7-hydroxy-2-methyl-8-[(2-methylpiperidin-1-yl)methyl]-4H-chromen-4-one (**7c**). Yield 79%, m.p. 204–205 °C, colorless. LC-MS: m/z 421.2 [M + H]$^+$. ^{1}H-NMR (400 MHz, CDCl$_3$): δ ppm 9.83 (s, 1H), 8.08 (d, J = 8.8 Hz, 1H), 8.03 (d, J = 8.1 Hz, 1H), 7.96 (d, J = 7.9 Hz, 1H), 7.50–7.41 (m, 1H), 7.40–7.32 (m, 1H), 6.86 (d, J = 8.8 Hz, 1H), 4.48–4.23 (m, 1H), 3.90 (d, J = 15.0 Hz, 1H), 3.14–2.85 (m, 4H), 2.75–2.13 (m, 2H), 1.91–1.34 (m, 6H), 1.24 (d, J = 6.1 Hz, 3H); ^{13}C-NMR (125 MHz, CDCl$_3$): δ ppm 175.0, 167.9, 164.5, 160.5, 154.2, 151.7, 136.0, 126.3, 125.6, 124.7, 122.8, 121.3, 116.3, 115.5, 114.9, 107.4, 57.8, 54.5, 50.8, 35.4,

34.2, 25.6, 25.2, 21.9. Elemental analysis for $C_{24}H_{24}N_2O_3S$; Calc.: C, 68.55; H, 5.75; N, 6.66%. Found: C, 68.57; H, 5.73; N, 6.67%.

3-(1,3-Benzothiazol-2-yl)-7-hydroxy-2-methyl-8-[(3-methylpiperidin-1-yl)methyl)]-4H-chromen-4-one (**7d**). Yield 83%, m.p. 200–201 °C, colorless. LC-MS: *m/z* 421.0 [M + H]$^+$. ^{1}H-NMR (500 MHz, CDCl$_3$): δ ppm 8.11 (d, *J* = 8.8 Hz, 1H), 8.03 (d, *J* = 8.1 Hz, 1H), 7.96 (d, *J* = 7.9 Hz, 1H), 7.53–7.43 (m, 2H), 7.41–7.32 (m, 1H), 6.89 (d, *J* = 8.8 Hz, 1H), 4.03 (s, 2H), 3.02 (s, 3H), 3.00–2.85 (m, 1H), 2.14–1.56 (m, 6H), 1.14–0.95 (m, 1H), 0.92 (d, *J* = 6.2 Hz, 3H). ^{13}C-NMR (125 MHz, CDCl$_3$): δ ppm 175.2, 167.9, 164.9, 160.5, 154.4, 151.8, 136.1, 126.7, 125.7, 124.8, 122.8, 121.4, 116.2, 115.7, 115.1, 107.0, 61.1, 54.4, 53.7, 32.3, 25.4, 21.9, 19.5. Elemental analysis for $C_{24}H_{24}N_2O_3S$; Calc.: C, 68.55; H, 5.75; N, 6.66%. Found: C, 68.57; H, 5.73; N, 6.67%.

3-(1,3-Benzothiazol-2-yl)-7-hydroxy-2-methyl-8-[(4-methylpiperidin-1-yl)methyl]-4H-chromen-4-one (**7e**). Yield 85%, m.p. 216–218 °C, colorless. LC-MS: *m/z* 421.0 [M + H]$^+$. ^{1}H-NMR (400 MHz, CDCl$_3$): δ ppm 8.13 (d, *J* = 8.8 Hz, 1H), 8.06 (d, *J* = 8.1 Hz, 1H), 7.99 (d, *J* = 7.8 Hz, 1H), 7.54–7.46 (m, 1H), 7.45–7.34 (m, 1H), 6.92 (d, *J* = 8.8 Hz, 1H), 4.07 (s, 2H), 3.16–3.05 (m, 2H), 3.04 (s, 3H), 2.43–2.20 (m, 2H), 1.85–1.72 (m, 2H), 1.60–1.48 (m, 1H), 1.45–1.30 (m, 2H), 1.00 (d, *J* = 6.4 Hz, 3H). ^{13}C-NMR (100 MHz, CDCl$_3$): δ ppm 175.0, 168.0, 164.8, 160.4, 154.3, 151.7, 136.0, 126.5, 125.7, 124.8, 122.8, 121.3, 116.1, 115.5, 115.0, 107.0, 54.2, 53.6, 34.0, 30.4, 22.0, 21.6. Elemental analysis for $C_{24}H_{24}N_2O_3S$; Calc.: C, 68.55; H, 5.75; N, 6.66%. Found: C, 68.56; H, 5.73; N, 6.65%.

3-(1,3-Benzothiazol-2-yl)-7-hydroxy-2-methyl-8-(morpholin-4-ylmethyl)-4H-chromen-4-one (**7f**), pale yellow crystals. Yield 88%, m.p. 243–244 °C. LC-MS: *m/z* 409.2 [M + H]$^+$. ^{1}H-NMR (400 MHz, CDCl$_3$): δ ppm 8.14 (d, *J* = 8.8 Hz, 1H), 8.05 (d, *J* = 8.0 Hz, 1H), 7.98 (d, *J* = 7.8 Hz, 1H), 7.54–7.45 (m, 1H), 7.44–7.35 (m, 1H), 6.92 (d, *J* = 8.8 Hz, 1H), 4.07 (s, 2H), 3.97–3.67 (m, 4H), 3.04 (s, 3H), 2.88–2.53 (m, 4H). ^{13}C-NMR (100 MHz, CDCl$_3$): δ ppm 175.1, 168.1, 163.8, 160.3, 154.5, 151.7, 136.0, 127.1, 125.8, 124.9, 122.9, 121.4, 116.1, 115.8, 115.6, 106.5, 66.7, 54.2, 53.2, 22.0. Elemental analysis for $C_{22}H_{20}N_2O_4S$; Calc.: C, 64.69; H, 4.94; N, 6.86%. Found: C, 64.67; H, 4.96; N, 6.85%.

3-(1,3-Benzothiazol-2-yl)-7-hydroxy-2-methyl-8-[(4-methylpiperazin-1-yl)methyl]-6-propyl-4H-chromen-4-one (**7g**), colorless. Yield 68%, m.p. 230–231 °C. LC-MS: *m/z* 464.2 [M + H]$^+$. ^{1}H-NMR (400 MHz, CDCl$_3$): δ ppm 8.04 (d, *J* = 8.1 Hz, 1H), 8.00–7.94 (m, 2H), 7.51–7.43 (m, 1H), 7.41–7.34 (m, 1H), 4.06 (s, 2H), 3.03 (s, 3H), 2.99–2.40 (m, 10H), 2.35 (s, 3H), 1.80–1.59 (m, 2H), 0.98 (t, *J* = 7.3 Hz, 3H). ^{13}C-NMR (125 MHz, CDCl$_3$): δ ppm 175.0, 167.8, 162.4, 160.5, 152.8, 151.6, 136.0, 129.5, 125.6, 125.3, 124.6, 122.7, 121.2, 115.3, 114.6, 106.0, 54.7, 53.8, 52.6, 45.9, 31.7, 22.5, 22.0, 14.0. Elemental analysis for $C_{26}H_{29}N_3O_3S$; Calc.: C, 67.36; H, 6.31; N, 9.06%. Found: C, 67.32; H, 6.29; N, 9.07%.

2-Amino-3-(1,3-benzothiazol-2-yl)-7-hydroxy-8-[(4-methylpiperazin-1-yl)methyl]-4H-chromen-4-one (**7h**), yellow. Yield 59%, m.p. 248–250 °C. LC-MS: *m/z* 423.2 [M + H]$^+$. ^{1}H-NMR (400 MHz, DMSO-d_6): δ ppm 10.76 (s, 1H), 9.39 (s, 1H), 8.02 (d, *J* = 7.4 Hz, 1H), 7.94 (d, *J* = 7.8 Hz, 1H), 7.89 (d, *J* = 8.4 Hz, 1H), 7.50–7.41 (m, 1H), 7.38–7.29 (m, 1H), 6.84 (d, *J* = 8.3 Hz, 1H), 4.02 (s, 2H), 2.70–2.57 (m, 4H), 2.46–2.29 (m, 4H), 2.18 (s, 3H). J^{13}C-NMR (125 MHz, CDCl$_3$): δ ppm 172.3, 163.3, 162.7, 162.3, 151.2, 149.9, 132.9, 125.7, 125.3, 123.6, 121.3, 120.5, 113.7, 113.0, 108.1, 91.7, 54.4, 52.1, 51.5, 45.5. Elemental analysis for $C_{22}H_{24}N_4O_3S$; Calc.: C, 62.54; H, 5.25; N, 13.26%. Found: C, 62.52; H, 5.27; N, 13.24%.

3-(1,3-Benzothiazol-2-yl)-7-hydroxy-8-{[4-(2-hydroxyethyl)piperazin-1-yl]methyl}-2-methyl-6-propyl-4H-chromen-4-one (**7i**), colorless. Yield 76%, m.p. 203–204 °C. LC-MS: *m/z* 494.0 [M + H]$^+$. ^{1}H-NMR (500 MHz, CDCl$_3$): δ ppm 8.05 (d, *J* = 8.1 Hz, 1H), 8.01–7.96 (m, 2H), 7.52–7.44 (m, 1H), 7.45–7.34 (m, 1H), 4.08 (s, 2H), 3.69–3.62 (m, 2H), 3.04 (s, 3H), 3.00–2.28 (m, 13H), 1.75–1.60 (m, 2H), 0.99 (t, *J* = 7.3 Hz, 3H). ^{13}C-NMR (125 MHz, CDCl$_3$): δ ppm 175.2, 167.8, 162.4, 160.7, 153.0, 151.8, 136.1, 129.6, 125.7, 125.7, 124.8, 122.8, 121.4, 115.6, 114.8, 106.0, 59.2, 57.9, 53.8, 52.7, 52.6, 31.8, 22.6, 22.0, 14.1. Elemental analysis for $C_{27}H_{31}N_3O_4S$; Calc.: C, 65.70; H, 6.33; N, 8.51%. Found: C, 65.68; H, 6.35; N, 8.53%.

3-(1,3-Benzothiazol-2-yl)-6-ethyl-7-hydroxy-8-[(1,3,3-trimethyl-6-azabicyclo [3.2.1]oct-6-yl)methyl]-4H-chromen-4-one (**7j**), pale yellow. Yield 84%, m.p. 183–185 °C. LC-MS: *m/z* 489.2 [M + H]$^+$. ^{1}H-NMR (300 MHz, CDCl$_3$): δ ppm 9.14 (s, 1H), 8.07 (s, 1H), 8.05–7.94

(m, 2H), 7.55–7.44 (m, 1H), 7.42–7.33 (m, 1H), 4.31 (d, *J* = 14.3 Hz, 1H), 4.04 (d, *J* = 14.3 Hz, 1H), 3.36–3.28 (m, 1H), 3.27–3.16 (m, 1H), 2.83–2.62 (m, 2H), 2.33–2.24 (m, 1H), 1.93–1.71 (m, 2H), 1.59–1.37 (m, 2H), 1.38–1.23 (m, 7H), 1.13 (s, 4H), 0.96 (s, 3H). ^{13}C-NMR (125 MHz, CDCl$_3$): δ ppm 174.4, 164.4, 159.5, 155.1, 153.5, 151.8, 136.4, 132.1, 126.1, 124.7, 124.5, 122.4, 121.7, 117.6, 115.2, 108.0, 64.8, 62.6, 54.2, 51.5, 44.0, 41.7, 40.7, 36.9, 32.2, 29.6, 25.9, 22.9, 13.8. Elemental analysis for C$_{29}$H$_{32}$N$_2$O$_3$S; Calc.: C, 71.26; H, 6.60; N, 5.73%. Found: C, 71.25; H, 6.58; N, 5.76%.

3-(1,3-Benzothiazol-2-yl)-7-hydroxy-2-methyl-8-[(1,3,3-trimethyl-6-azabicyclo [3.2.1]oct-6-yl)methyl]-4H-chromen-4-one (**7k**), colorless. Yield 87%, m.p. 158–159 °C. LC-MS: *m/z* 475.2 [M + H]$^+$. ^{1}H-NMR (400 MHz, CDCl$_3$): δ ppm 10.43 (s, 1H), 8.12 (d, *J* = 8.8 Hz, 1H), 8.04 (d, *J* = 8.0 Hz, 1H), 7.97 (d, *J* = 7.9 Hz, 1H), 7.52–7.43 (m, 1H), 7.43–7.33 (m, 1H), 6.91 (d, *J* = 8.8 Hz, 1H), 4.28 (d, *J* = 14.5 Hz, 1H), 4.00 (d, *J* = 14.5 Hz, 1H), 3.34 (d, *J* = 11.0 Hz, 1H), 3.27–3.16 (m, 1H), 3.02 (s, 3H), 2.32–2.22 (m, 1H), 1.92–1.78 (m, 2H), 1.59–1.48 (m, 1H), 1.47–1.40 (m, 1H), 1.36–1.28 (m, 2H), 1.26 (s, 3H), 1.14 (s, 3H), 0.97 (s, 3H); ^{13}C-NMR (125 MHz, CDCl$_3$): δ ppm 175.0, 167.8, 165.6, 160.5, 154.1, 151.7, 136.1, 126.7, 125.7, 124.8, 122.8, 121.3, 116.3, 115.5, 114.7, 108.1, 65.1, 62.7, 54.4, 51.5, 43.9, 41.7, 40.6, 36.9, 32.1, 29.6, 25.9, 22.0. Elemental analysis for C$_{28}$H$_{30}$N$_2$O$_3$S; Calc.: C, 70.86; H, 6.37; N, 5.90%. Found: C, 70.90; H, 6.38; N, 5.88%.

Ethyl 3-(1,3-benzothiazol-2-yl)-6-ethyl-7-hydroxy-4-oxo-8-[(1,3,3-trimethyl-6-azabicyclo[3.2.1]oct-6-yl)methyl]-4H-chromene-2-carboxylate (**7l**), colorless. Yield 78%, m.p. 153–154 °C. LC-MS: *m/z* 561.2 [M + H]$^+$. ^{1}H-NMR (400 MHz, CDCl$_3$): δ ppm 12.15 (s, 1H), 8.04 (s, 1H), 8.01–7.92 (m, 2H), 7.52–7.44 (m, 1H), 7.39 (t, *J* = 7.5 Hz, 1H), 4.51 (q, *J* = 7.2 Hz, 2H), 4.32 (d, *J* = 14.4 Hz, 1H), 4.05 (d, *J* = 14.4 Hz, 1H), 3.35 (d, *J* = 11.0 Hz, 1H), 3.28–3.17 (m, 1H), 2.88–2.63 (m, 2H), 2.31 (d, *J* = 11.0 Hz, 1H), 1.96–1.70 (m, 2H), 1.60–.50 (m, 1H), 1.48–1.39 (m, 1H), 1.35–1.28 (m, 8H), 1.27 (s, 3H), 1.13 (s, 3H), 0.97 (s, 3H); ^{13}C-NMR (125 MHz, CDCl$_3$): δ ppm 174.6, 165.2, 162.2, 157.7, 153.9, 152.9, 151.6, 136.6, 132.7, 126.0, 125.0, 124.4, 122.9, 121.7, 114.9, 114.5, 107.6, 64.7, 63.1, 62.6, 54.1, 51.5, 43.8, 41.7, 40.6, 36.9, 32.2, 29.6, 25.8, 22.9, 13.9, 13.7. Elemental analysis for C$_{32}$H$_{36}$N$_2$O$_5$S; Calc.: C, 68.55; H, 6.47; N, 5.00%. Found: C, 68.53; H, 6.51; N, 5.03%.

2-Amino-6-ethyl-7-hydroxy-3-(4-methyl-1,3-thiazol-2-yl)-8-(piperidin-1-ylmethyl)-4H-chromen-4-one (**7m**), yellow. Yield 49%, m.p. 174–175 °C. LC-MS: *m/z* 400.2 [M + H]$^+$. ^{1}H-NMR (500 MHz, CDMSO-*d$_6$*): δ ppm 10.47 (s, 1H), 9.00 (s, 1H), 7.70 (s, 1H), 6.99 (s, 1H), 4.05 (s, 2H), 2.66–2.51 (m, 6H), 2.40 (s, 3H), 1.67–1.55 (m, 4H), 1.53–1.42 (m, 2H), 1.17 (t, *J* = 7.5 Hz, 3H). ^{13}C-NMR (125 MHz, CDCl$_3$): δ ppm 173.5, 162.5, 161.6, 161.5, 149.6, 148.5, 129.4, 124.1, 113.2, 111.7, 106.0, 93.6, 54.5, 53.9, 25.7, 23.8, 22.7, 17.2, 13.7. Elemental analysis for C$_{21}$H$_{25}$N$_3$O$_3$S; Calc.: C, 63.13; H, 6.31; N, 10.52%. Found: C, 63.10; H, 6.15; N, 10.50%.

3.2.4. General Procedure for Synthesis of Coumarin Aminomethyl Derivatives **10,11**

A stirring mixture of the corresponding 3-hetarylcoumarin **9** or **10a,b** chromone (1 mmol) and aminal (1.2 mmol) in 1,4-dioxane (5 mL) was refluxed for 6–8 h. The reaction mixture was cooled, diluted with 10 mL of hexane. The formed precipitate was filtered off, dried, and re-crystallized from toluene-hexane mixture to furnish the desired chromone Mannich bases **7**.

3-(1,3-Benzothiazol-2-yl)-8-{[bis(2-hydroxyethyl)amino]methyl}-7-hydroxy-2H-chromen-2-one (**10a**). Yield 56%, m.p. 186–187 °C, yellow. LC-MS: *m/z* 413.2 [M + H]$^+$. ^{1}H-NMR (400 MHz, DMSO-*d$_6$*): δ ppm 9.01 (s, 1H), 8.09 (d, *J* = 7.9 Hz, 1H), 7.98 (d, *J* = 8.1 Hz, 1H), 7.74 (d, *J* = 8.7 Hz, 1H), 7.54–7.48 (m, 1H), 7.45–7.32 (m, 1H), 6.69 (d, *J* = 8.6 Hz, 1H), 4.23 (s, 2H), 3.65 (t, *J* = 5.5 Hz, 4H), 2.87 (t, *J* = 5.5 Hz, 4H). ^{13}C-NMR (125 MHz, CDCl$_3$): δ ppm 168.4, 160.9, 159.8, 153.9, 152.1, 142.9, 135.4, 130.8, 126.3, 124.6, 122.0, 121.9, 116.0, 111.4, 109.6, 107.4, 57.3, 55.1, 49.8. Elemental analysis for C$_{21}$H$_{20}$N$_2$O$_5$S; Calc.: C, 61.15; H, 4.89; N, 6.79%. Found: C, 61.12; H, 4.91; N, 6.77%.

3-(1,3-Benzothiazol-2-yl)-8-[(3,3-dimethylpiperidin-1-yl)methyl]-7-hydroxy-2H-chromen-2-one (**10b**). Yield 85%, m.p. 188–189 °C, green (fluorescent). LC-MS: *m/z* 421.0 [M + H]$^+$. ^{1}H-NMR (500 MHz, CDCl$_3$): δ ppm 8.97 (s, 1H), 8.05 (d, *J* = 8.1 Hz, 1H), 7.95 (d, *J* = 7.8 Hz,

1H), 7.54–7.47 (m, 2H), 7.41–7.35 (m, 1H), 6.83 (d, *J* = 8.6 Hz, 1H), 4.17–3.95 (m, 2H), 3.19–2.45 (m, 2H), 2.32–1.91 (m, 1H), 1.91–1.16 (m, 5H), 1.02 (s, 6H). ^{13}C-NMR (125 MHz, CDCl$_3$): δ ppm 166.0, 161.0, 160.4, 153.5, 152.6, 142.8, 136.6, 130.1, 126.4, 125.0, 122.6, 121.8, 115.5, 114.8, 111.3, 107.5, 65.8, 54.7, 53.8, 36.7, 31.2, 21.9. Elemental analysis for C$_{24}$H$_{24}$N$_2$O$_3$S; Calc.: C, 68.55; H, 5.75; N, 6.66%. Found: C, 68.52; H, 5.77; N, 6.67%.

3-(1,3-Benzothiazol-2-yl)-7-hydroxy-8-{[4-(2-hydroxyethyl)piperazin-1-yl]methyl}-2H-chromen-2-one (**10c**). Yield 64%, m.p. 207–208 °C, yellow. LC-MS: *m/z* 438.0 [M + H]$^+$. ^{1}H-NMR (400 MHz, DMSO-*d$_6$*): δ ppm 9.06 (s, 1H), 8.11 (d, *J* = 7.9 Hz, 1H), 8.00 (d, *J* = 8.1 Hz, 1H), 7.79 (d, *J* = 8.6 Hz, 1H), 7.56–7.48 (m, 1H), 7.45–7.37 (m, 1H), 6.79 (d, *J* = 8.6 Hz, 1H), 3.99 (s, 2H), 3.50 (t, *J* = 6.0 Hz, 2H), 2.80–2.53 (m, 8H), 2.45–2.36 (m, 2H). ^{13}C-NMR (125 MHz, DMSO-*d$_6$*): δ ppm 165.9, 160.6, 159.7, 153.7, 152.0, 142.9, 135.5, 130.8, 126.4, 124.8, 122.0, 118.8, 115.2, 112.7, 110.4, 107.4, 59.8, 58.4, 52.6, 51.9, 51.7. Elemental analysis for C$_{23}$H$_{23}$N$_3$O$_4$S; Calc.: C, 63.14; H, 5.30; N, 9.60%. Found: C, 63.12; H, 5.28; N, 9.63%.

7-Hydroxy-8-{[4-(2-hydroxyethyl)piperazin-1-yl]methyl}-3-(4-methyl-1,3-thiazol-2-yl)-2H-chromen-2-one (**11a**). Yield 58%, m.p. 157–159 °C, yellow. LC-MS: *m/z* 402.2 [M + H]$^+$. ^{1}H-NMR (500 MHz, CDCl$_3$): δ ppm 8.74 (s, 1H), 7.45 (d, *J* = 8.6 Hz, 1H), 7.04–6.98 (m, 1H), 6.81 (d, *J* = 8.6 Hz, 1H), 4.11 (s, 2H), 3.68–3.60 (m, 2H), 3.20–2.53 (m, 10H), 2.52 (s, 3H). ^{13}C-NMR (125 MHz, CDCl$_3$): δ ppm 163.8, 160.2, 159.2, 152.9, 152.8, 139.9, 129.6, 116.4, 115.8, 115.0, 111.8, 107.4, 59.3, 58.0, 53.7, 52.8, 52.6, 17.3. Elemental analysis for C$_{20}$H$_{23}$N$_3$O$_4$S; Calc.: C, 59.83; H, 5.77; N, 10.47%. Found: C, 59.85; H, 5.79; N, 10.44%.

3-[4-(4-Bromophenyl)-1,3-thiazol-2-yl]-7-hydroxy-8-{[4-(2-hydroxyethyl)piperazin-1-yl]methyl}-2H-chromen-2-one (**11b**). Yield 71%, m.p. 224–225 °C, colorless. LC-MS: *m/z* 542.0 [M + H]$^+$. ^{1}H-NMR (300 MHz, CDCl$_3$): δ ppm 8.88 (s, 1H), 7.88 (d, *J* = 8.5 Hz, 2H), 7.62 (s, 1H), 7.58 (d, *J* = 8.6 Hz, 2H), 7.52 (d, *J* = 8.6 Hz, 1H), 6.85 (d, *J* = 8.6 Hz, 1H), 4.13 (s, 2H), 3.68–3.59 (m, 2H), 3.03–2.29 (m, 10H). ^{13}C-NMR (100 MHz, CDCl$_3$): δ ppm 164.1, 160.2, 159.8, 154.1, 152.9, 140.5, 133.5, 131.9, 129.7, 128.0, 122.2, 115.8, 115.5, 115.1, 111.7, 107.4, 59.2, 57.9, 53.7, 52.8, 52.6. Elemental analysis for C$_{25}$H$_{24}$BrN$_3$O$_4$S; Calc.: C, 55.35; H, 4.46; N, 7.75%. Found: C, 55.32; H, 4.49; N, 7.73%.

3-[4-(4-Bromophenyl)-1,3-thiazol-2-yl]-7-hydroxy-8-[(2-methylpiperidin-1-yl)methyl]-2H-chromen-2-one (**11c**). Yield 68%, m.p. 184–186 °C, yellow. LC-MS: *m/z* 511.0 [M + H]$^+$. ^{1}H-NMR (300 MHz), δ 11.31 (s, 1H), 8.85 (s, 1H), 7.87 (d, *J* = 8.5 Hz, 2H), 7.61–7.54 (m, 3H), 7.47 (d, *J* = 8.6 Hz, 1H), 6.79 (d, *J* = 8.6 Hz, 1H), 4.55–4.23 (m, 1H), 4.08–3.91 (m, 1H), 3.20–2.15 (m, 3H), 1.91–1.34 (m, 6H), 1.25 (d, *J* = 5.5 Hz, 3H). ^{13}C-NMR (125 MHz, CDCl$_3$–TFA 1:1): δ ppm 165.1, 160.6, 155.7, 148.4, 148.1, 135.8, 133.8, 129.5, 128.7, 127.7, 125.1, 118.1, 116.8, 112.7, 109.0, 105.0, 64.4, 54.0, 47.4, 32.1, 23.3, 21.8, 18.1. Elemental analysis for C$_{25}$H$_{23}$BrN$_2$O$_3$S; Calc.: C, 58.71; H, 4.53; N, 5.48%. Found: C, 58.68; H, 4.50; N, 5.50%.

3-[4-(4-Bromophenyl)-1,3-thiazol-2-yl]-7-hydroxy-8-[(3-methylpiperidin-1-yl)methyl]-2H-chromen-2-one (**11d**). Yield 83%, m.p. 216–217 °C, yellow. LC-MS: *m/z* 511.0 [M + H]$^+$. ^{1}H-NMR (300 MHz, CDCl$_3$): δ ppm 11.45 (s, 1H), 8.84 (s, 1H), 7.87 (d, *J* = 8.5 Hz, 2H), 7.61–7.53 (m, 3H), 7.48 (d, *J* = 8.6 Hz, 1H), 6.81 (d, *J* = 8.6 Hz, 1H), 4.06 (s, 2H), 3.10–2.85 (m, 2H), 2.39–1.52 (m, 6H), 1.15–0.73 (m, 4H); ^{13}C-NMR (125 MHz, DMSO-*d$_6$*): δ ppm 162.4, 159.4, 159.2, 154.5, 153.2, 140.5, 133.3, 132.8, 131.9, 128.4, 121.6, 117.4, 115.2, 114.1, 111.7, 103.6, 58.5, 52.4, 48.7, 29.7, 29.0, 22.7, 18.8. Elemental analysis for C$_{25}$H$_{23}$BrN$_2$O$_3$S; Calc.: C, 58.71; H, 4.53; N, 5.48%. Found: C, 58.72; H, 4.51; N, 5.50%.

3-[4-(4-Bromophenyl)-1,3-thiazol-2-yl]-7-hydroxy-8-[(4-methylpiperidin-1-yl)methyl]-2H-chromen-2-one (**11e**). Yield 85%, m.p. 229–230 °C, yellow. LC-MS: *m/z* 511.0 [M + H]$^+$. ^{1}H-NMR (400 MHz, DMSO-*d$_6$*): δ ppm 8.94 (s, 1H), 8.18 (s, 1H), 8.03 (d, *J* = 8.1 Hz, 2H), 7.73 (d, *J* = 8.7 Hz, 1H), 7.66 (d, *J* = 8.2 Hz, 2H), 6.75 (d, *J* = 8.7 Hz, 1H), 4.07 (s, 2H), 3.08–2.97 (m, 2H), 2.48–2.36 (m, 2H), 1.79–1.65 (m, 2H), 1.58–1.42 (m, 1H), 1.33–1.16 (m, 2H), 0.94 (d, *J* = 6.1 Hz, 3H). ^{13}C-NMR (125 MHz, CDCl$_3$–TFA 1:1): δ ppm 165.3, 164.9, 160.6, 155.6, 148.4, 148.0, 135.8, 133.8, 128.7, 127.7, 125.0, 118.0, 116.8, 112.5, 108.8, 104.5, 55.3, 50.3, 31.6, 29.0, 20.3. Elemental analysis for C$_{25}$H$_{23}$BrN$_2$O$_3$S; Calc.: C, 58.71; H, 4.53; N, 5.48%. Found: C, 58.70; H, 4.54; N, 5.51%.

7-Hydroxy-3-(4-methyl-1,3-thiazol-2-yl)-8-[(1,3,3-trimethyl-6-azabicyclo [3.2.1]oct-6-yl)methyl]-2H-chromen-2-one (**11f**). Yield 70%, m p. 159–160 °C, yellow (fluorescent). LC-MS: m/z 425.0 [M + H]$^+$. ^{1}H-NMR (500 MHz, CDCl$_3$): δ ppm 8.73 (s, 1H), 7.44 (d, *J* = 8.6 Hz, 1H), 6.99 (s, 1H), 6.80 (d, *J* = 8.6 Hz, 1H), 4.37 (d, *J* = 14.6 Hz, 1H), 4.07 (d, *J* = 14.6 Hz, 1H), 3.36 (d, *J* = 11.2 Hz, 1H), 3.30–3.19 (m, 1H), 2.52 (s, 3H), 2.30 (d, *J* = 11.2 Hz, 1H), 1.96–1.76 (m, 2H), 1.53 (d, *J* = 14.0 Hz, 1H), 1.42 (d, *J* = 13.7 Hz, 1H), 1.32 (dd, *J* = 14.3, 2.2 Hz, 1H), 1.28 (d, *J* = 11.5 Hz, 1H), 1.24 (s, 3H), 1.12 (s, 3H), 0.95 (s, 3H). ^{13}C-NMR (125 MHz, CDCl$_3$): δ ppm 166.6, 160.5, 159.6, 152.8, 152.8, 140.4, 129.8, 116.0, 115.7, 114.6, 110.7, 108.1, 64.9, 63.1, 54.8, 51.5, 43.8, 41.7, 40.6, 36.9, 32.1, 29.6, 25.8, 17.4. Elemental analysis for C$_{24}$H$_{28}$rN$_2$O$_3$S; Calc.: C, 67.90; H, 6.65; N, 6.60%. Found: C, 67.88; H, 6.67; N, 6.63%.

4. Biological Evaluation

4.1. Cell Viability Studies

A set of 25 compounds was tested for cell viability studies using MTT assay, in HCT116 and HeLa cell lines. All experiments were carried out in triplicate as per previously reported methods [53,54]. For the viability studies, HCT116 and HeLa cells were seeded at the count of 7×10^3 cells per well in a transparent 96-well plates, and incubated for 24 h at 37 °C, in a humidified incubator with 5% CO$_2$. Following this, the cells were treated with the compounds at a final concentration of 10 μM and incubated further for 72 h at 37 °C. After incubation, MTT [3-(4,5-Dimethyl-2-thiazolyl)-2,5-diphenyl tetrazolium bromide] was added at a final concentration of 0.5 mg/mL. The cells were further incubated for 4 h at 37 °C in an incubator. The formazan crystals formed were dissolved using 50 μL of DMSO. Thereafter, the absorbance was measured at 570 nm using the PerkinElmer EnVision Multilabel Reader (Perkin Elmer, Inc., Waltham, MA, USA). The cells treated with DMSO were used as a control for all the experiments. Both the cell lines showed viability ≤ 50% for three compounds in the initial screening, namely **2c**, **7h** and **7l**. Hence, these three compounds were selected from the initial screening and were sensitized against HCT116 and HeLa, across a dose range of 0–100 μM by performing another cell viability assay. Finally, the results obtained were plotted using Graphpad Prism 8.0.2 to obtain the respective IC$_{50}$ values.

4.2. Immunoblot Assay

The immunoblot assay was carried out as per previous reports [2]. HCT116 and HeLa cells were seeded at the count of 0.5×10^5 cells per ml in a 6-well plate and incubated overnight at 37 °C, in a humidified CO$_2$ incubator. For this assay, the cells were treated with the hit compounds with their concentration range approximately equal to their IC$_{50}$ values (Table 3), and incubated for 1 h at 37 °C. After the incubation, the cells were given UV radiation energy via UVP cross linker at 50 mJ/cm^2 and further incubated for 1 h at 37 °C. The media was stored before UV radiation and added back after the treatment. The cells were then trypsinized, washed with ice cold 1X PBS, and lysed with RIPA buffer. The cell lysates were isolated by centrifugation at 4 °C, 13,500 rpm for 10 min. The protein concentration was normalized by Bradford assay. The samples were loaded on SDS-PAGE gel and subjected to immunoblotting. β-actin was taken as a loading control in the experiment.

Table 3. Concentration of compounds **2c**, **7h** and **7l** for immunoblot assay in HCT116 and HeLa cell lines.

Sl. No.	Compound	Concentration for Blot (μM)	
		HCT116	HeLa
1	**2c**	3.6	2.6
2	**7h**	6.5	4.0
3	**7l**	2.5	2.6

Further, to identify the pattern of inhibition of Chk1 phosphorylation, the immunoblot assay was repeated for a range of concentrations of the compounds **2c**, **7h**, and **7l** in HeLa cell line against Chk1 and pChk1 antibodies. The experiments were conducted in a similar way for a concentration range of 2 μM, 5 μM and 10 μM. β-actin was taken as a loading control in the experiment.

4.3. Molecular Docking

In the present study, the compounds **2c**, **7h** and **7l** were subjected to molecular docking studies at the Torin2 binding site of homology modelled ATR kinase domain [55], using the Glide module (XP) of Maestro 12.7.156 version of Schrödinger software [56]. The homology modelled ATR kinase domain was further prepared for molecular docking, using the Protein Preparation Wizard by including Epik state penalties (pH 7.0 ± 2.0), and by performing the minimization using 0.3 Å RMSD and OPLS4 force field [57–59]. Further, the compounds **2c**, **7h** and **7l** were included in the project using the 2D sketcher option in the software, following which the 3D structures were incorporated in the workspace. The standard molecule for the study was selected to be Torin2, the standard inhibitor in the modelled structure, which is a well-known mTOR and ATR/ATM inhibitor known for its potency against the p-Chk1 Ser 317 and p70 S6K Thr 389 substrates in the DDR pathway through cell studies. The ligands were then prepared using the LigPrep module [57].

The ligand preparation was followed by receptor grid generation, wherein the grid was generated using the Glide module, by selecting the Torin2 ligand from the minimized protein structure. Ligand docking for the standard molecule and the synthesized compounds was conducted in the Glide XP (Extra Precision) module [56].

The docking results were analyzed in the XP Visualizer tool, wherein the binding energies were analyzed using the docking score instead of GlideScore, since the Epik state penalties were included during the protein and ligand preparations. The best pose of each of the compounds **2c**, **7h** and **7l** with higher negative value of DockScore were considered for the study.

5. Conclusions

A series of benzothiazole and chromone derivatives were synthesized and evaluated for their anticancer activity as inhibitors of ATR kinase. Cell viability of a set of 25 compounds was performed using MTT assay in HCT116 and HeLa cell lines, involving 72 h incubation of the compounds at a final concentration of 10 μM. Cells incubated with compounds **2c**, **7h** and **7l** were found to show a viability ≤50, and were taken forward for dose–response studies. The three compounds showed IC$_{50}$ values in micromolar range. Among all the compounds tested, **7l** had the best IC$_{50}$ values in both the cell lines. Compounds **2c** and **7l** were found to be equally cytotoxic towards both the cell lines, namely, HCT116 and Hela, while compound **7h** showed better cytotoxicity towards HeLa cell line.

To further identify the inhibitory potential of the synthesized compounds in the DNA damage response (DDR) signalling pathway, an immunoblot assay was carried out for these three compounds in order to analyze the inhibition of phosphorylation of Chk1 at Ser 317 in HeLa and HCT116 cells. Compound **7h** showed inhibition of pChk1 at Ser 317 in HeLa cells at a concentration of 3.995 μM. Further analysis for Chk1 and pChk1 expression was analyzed in Hela cells by treatment against all the three compounds at a range of concentrations such as 2, 5 and 10 μM, wherein compound **7h** showed Chk1 inhibition at 2 and 5 μM, while pChk1 expression was observed for compound **7l** at a concentration of 5 μM. The binding interactions of the compounds with the ATR kinase domain were studied through molecular docking, wherein compound **2c**, **7h** and **7l** showed binding interactions similar and/or lesser than the standard ligand Torin2. Thus, these compounds can serve as starting point for further modifications in order to improve the activity.

References

1. Srinivas, U.S.; Tan, B.W.Q.; Vellayappan, B.A.; Jeyasekharan, A.D. ROS and the DNA damage response in cancer. *Redox Biol.* **2019**, *25*, 101084. [CrossRef]
2. Bhakuni, R.; Shaik, A.; Priya, B.; Kirubakaran, S. Characterization of SPK 98, a Torin2 analog, as ATR and mTOR dual kinase inhibitor. *Bioorg. Med. Chem. Lett.* **2020**, *30*, 127517. [CrossRef] [PubMed]
3. Dietlein, F.; Thelen, L.; Reinhardt, H.C. Cancer-specific defects in DNA repair pathways as targets for personalized therapeutic approaches. *Trends Genet.* **2014**, *30*, 326–339. [CrossRef] [PubMed]
4. Fokas, E.; Prevo, R.; Hammond, E.M.; Brunner, T.B.; McKenna, W.G.; Muschel, R.J. Targeting ATR in DNA damage response and cancer therapeutics. *Cancer Treat. Rev.* **2014**, *40*, 109–117. [CrossRef] [PubMed]
5. Cilibrasi, V.; Spanò, V.; Bortolozzi, R.; Barreca, M.; Raimondi, M.V.; Rocca, R.; Maruca, A.; Montalbano, A.; Alcaro, S.; Ronca, R.; et al. Synthesis of 2H-Imidazo[2′,1′:2,3] [1,3]thiazolo[4,5-e]isoindol-8-yl-phenylureas with promising therapeutic features for the treatment of acute myeloid leukemia (AML) with FLT3/ITD mutations. *Eur. J. Med. Chem.* **2022**, *235*, 114292. [CrossRef] [PubMed]
6. Morsy, M.A.; Ali, E.M.; Kandeel, M.; Venugopala, K.N.; Nair, A.B.; Greish, H.; El-Daly, M. Screening and Molecular Docking of Novel Benzothiazole Derivatives as Potential Antimicrobial Agents. *Antibiotics* **2020**, *9*, 221. [CrossRef]
7. Haroun, M.; Tratrat, C.; Petrou, A.; Geronikaki, A.; Ivanov, M.; Ciric, A.; Soković, M.; Nagaraja, S.; Venugopala, K.N.; Nair, A.B.; et al. Exploration of the Antimicrobial Effects of Benzothiazolylthiazolidin-4-One and In Silico Mechanistic Investigation. *Molecules* **2021**, *26*, 4061. [CrossRef]
8. Kumar, G.; Singh, N.P. Synthesis, anti-inflammatory and analgesic evaluation of thiazole/oxazole substituted benzothiazole derivatives. *Bioorg. Chem.* **2021**, *107*, 104608. [CrossRef]
9. Ugwu, D.I.; Okoro, U.C.; Ukoha, P.O.; Gupta, A.; Okafor, S.N. Novel anti-inflammatory and analgesic agents: Synthesis, molecular docking and in vivo studies. *J. Enzym. Inhib. Med. Chem.* **2018**, *33*, 405–415. [CrossRef]
10. Djuidje, E.N.; Barbari, R.; Baldisserotto, A.; Durini, E.; Sciabica, S.; Balzarini, J.; Liekens, S.; Vertuan, S.; Manfredini, S. Benzothiazole Derivatives as Multifunctional Antioxidant Agents for Skin Damage: Structure–Activity Relationship of a Scaffold Bearing a Five-Membered Ring System. *Antioxidants* **2022**, *11*, 407. [CrossRef]
11. Cabrera-Pérez, L.C.; Padilla-Martínez, I.I.; Cruz, A.; Mendieta-Wejebe, J.E.; Tamay-Cach, F.; Rosales-Hernández, M.C. Evaluation of a new benzothiazole derivative with antioxidant activity in the initial phase of acetaminophen toxicity. *Ar. J. Chem.* **2019**, *12*, 3871–3882. [CrossRef]
12. Kumar, K.R.; Karthik, K.N.S.; Begum, P.R.; Prasada, R.C.M.M. Synthesis, characterization and biological evaluation of benzothiazole derivatives as potential antimicrobial and analgesic agents. *Asian J. Res. Pharm. Sci.* **2017**, *7*, 115–119. [CrossRef]
13. Uremis, N.; Uremis, M.M.; Tolun, F.I.; Ceylan, M.; Doganer, A.; Kurt, A.H. Synthesis of 2-Substituted Benzothiazole Derivatives and Their In Vitro Anticancer Effects and Antioxidant Activities against Pancreatic Cancer Cells. *Anticancer Res.* **2017**, *37*, 6381–6389. [PubMed]
14. Irfan, A.; Batool, F.; Naqvi, S.Z.; Islam, A.; Osman, S.M.; Nocentini, A.; Alissa, S.A.; Supuran, C.T. Benzothiazole derivatives as anticancer agents. *J Enzym. Inhib. Med. Chem.* **2020**, *35*, 265–279. [CrossRef] [PubMed]
15. Islam, M.K.; Baek, A.-R.; Sung, B.; Yang, B.-W.; Choi, G.; Park, H.-J.; Kim, Y.-H.; Kim, M.; Ha, S.; Lee, G.-H.; et al. Synthesis, Characterization, and Anticancer Activity of Benzothiazole Aniline Derivatives and Their Platinum (II) Complexes as New Chemotherapy Agents. *Pharmaceuticals* **2021**, *14*, 832. [CrossRef]
16. Osmaniye, D.; Levent, S.; Karaduman, A.B.K.; Ilgın, S.; Özkay, Y.; Kaplancıklı, Z.A. Synthesis of New Benzothiazole Acylhydrazones as Anticancer Agents. *Molecules* **2018**, *23*, 1054. [CrossRef]

17. Asiri, Y.I.; Alsayari, A.; Muhsinah, A.B.; Mabkhot, Y.N.; Hassan, M.Z. Benzothiazoles as potential antiviral agents. *J. Pharm. Pharmacol.* **2020**, *72*, 1459–1480. [CrossRef]

18. Elamin, M.B.; Abd Elaziz, A.A.E.S.; Abdallah, E.M. Benzothiazole moieties and their derivatives as antimicrobial and antiviral agents: A mini-review. *Int. J. Res. Pharm. Sci.* **2020**, *3*, 3309–3315. [CrossRef]

19. Kumar, M.; Chung, S.-M.; Enkhtaivan, G.; Patel, R.V.; Shin, H.-S.; Mistry, B.M. Molecular Docking Studies and Biological Evaluation of Berberine–Benzothiazole Derivatives as an Anti-Influenza Agent via Blocking of Neuraminidase. *Int. J. Mol. Sci.* **2021**, *22*, 2368. [CrossRef]

20. Khyati Bhagdev, K.; Sarkar, S. Benzothiazole Moiety and Its Derivatives as Antiviral Agents. *Med. Sci. Forum* **2021**, *7*, 2–7.

21. Al-Masoudia, N.A.; Jafar, N.N.A.; Abbas, L.J.; Baqir, S.J.; Pannecouque, C. Synthesis and anti-HIV Activity of New Benzimidazole, Benzothiazole and Carbohyrazide Derivatives of the anti-Inflammatory Drug Indomethacin. *Z. Naturforsch.* **2011**, *66b*, 953–960. [CrossRef]

22. Petrou, A.; Eleftheriou, P.; Geronikaki, A.; Akrivou, M.G.; Vizirianakis, I. Novel thiazolidin-4-ones as potential non-nucleoside inhibitors of HIV-1 reverse transcriptase. *Molecules* **2019**, *24*, 3821. [CrossRef] [PubMed]

23. Ullah, S.; Mirza, S.; Salar, U.; Hussain, S.; Javaid, K.; Khan, K.M.; Khalil, R.; Atia-Tul-Wahab; Ul-Haq, Z.; Perveen, S.; et al. 2-Mercapto Benzothiazole Derivatives: As Potential Leads for the Diabetic Management. *Med. Chem.* **2020**, *16*, 826–840. [CrossRef] [PubMed]

24. Nath, R.; Shahar, Y.M.; Pathania, S.; Grover, G.; Debnath, B.; Akhtar, M.J. Synthesis and anticonvulsant evaluation of indoline derivatives of functionalized aryloxadiazole amine and benzothiazole acetamide. *J. Mol. Struct.* **2021**, *1228*, 129742. [CrossRef]

25. Khokra, S.L.; Arora, K.; Khan, S.A.; Kaushik, P.; Saini, R.; Husain, A. Synthesis, Computational Studies and Anticonvulsant Activity of Novel Benzothiazole Coupled Sulfonamide Derivatives. *Iran. J. Pharm. Res.* **2019**, *18*, 826–840.

26. Hadanu, R.; Idris, S.; Sutapa, I.W. QSAR analysis of benzothiazole derivatives of antimalarial compounds based on am1 semi-empirical method. *Indones. J. Chem.* **2015**, *15*, 86–92. [CrossRef]

27. Suresh, A.J.; Bharathi, K.; Surya, P.R. Design, Synthesis, Characterization and Biological Evaluation of Some Novel Benzothiazole Derivatives as Anti Tubercular Agents Targeting Glutamine Synthetase-I. And Cyclopropanemycolic acid synthase-2. *J. Pharm. Chem. Biol. Sci.* **2018**, *5*, 312–319.

28. Mehra, R.; Rajput, V.S.; Gupta, M.; Chib, R.; Kumar, A.; Wazir, P.; Ali Khan, I.; Nargotra, A. Benzothiazole Derivative as a Novel *Mycobacterium tuberculosis* Shikimate Kinase Inhibitor: Identification and Elucidation of Its Allosteric Mode of Inhibition. *J. Chem. Inf. Model.* **2016**, *56*, 930–940. [CrossRef]

29. Shahare, H.V.; Talele, G.S. Designing of benzothiazole derivatives as promising EGFR tyrosine kinase inhibitors: A pharmacoin-formatics study. *J. Biomol. Struct. Dyn.* **2020**, *38*, 1365–1374. [CrossRef]

30. Cao, S.; Cao, R.; Liu, X.; Luo, X.; Zhong, W. Design, Synthesis and Biological Evaluation of Novel Benzothiazole Derivatives as Selective PI3Kβ Inhibitors. *Molecules* **2016**, *21*, 876. [CrossRef]

31. Sugita, Y.; Takao, K.; Uesawa, Y.; Nagai, J.; Iijima, Y.; Sano, M.; Sakagami, H. Development of Newly Synthesized Chromone Derivatives with High Tumor Specificity against Human Oral Squamous Cell Carcinoma. *Medicines* **2020**, *7*, 50. [CrossRef] [PubMed]

32. Reis, J.; Gaspar, A.; Milhazes, N.; Borges, F. Chromone as a Privileged Scaffold in Drug Discovery: Recent Advances. *J. Med. Chem.* **2017**, *60*, 7941–7957. [CrossRef] [PubMed]

33. Bouhenna, M.M.; Mameri, N.; Pérez, M.V.; Talhi, O.; Bachari, K.; Silva, A.M.S.; Luyten, W. Anticancer Activity Study of Chromone and Coumarin Hybrids using Electrical Impedance Spectroscopy. Anticancer Agents. *Med. Chem.* **2018**, *18*, 854–864.

34. Zhan, Q.; Xu, Y.; Zhan, L.; Wang, B.; Guo, Y.; Wu, X.; Ai, W.; Song, Z.; Yu, F. Chromone Derivatives CM3a Potently Eradicate *Staphylococcus aureus* Biofilms by Inhibiting Cell Adherence. *Infect. Drug Resist.* **2021**, *14*, 979–986. [CrossRef]

35. Chu, Y.-C.; Chang, C.-H.; Liao, H.-R.; Fu, S.-L.; Chen, J.J. Anti-Cancer and Anti-Inflammatory Activities of Three New Chromone Derivatives from the Marine-Derived *Penicillium citrinum*. *Mar. Drugs* **2021**, *19*, 408–426. [CrossRef]

36. Matta, A.; Sharma, A.K.; Tomar, S.; Cao, P.; Kumar, S.; Balwani, S.; Ghosh, B.; Prasad, A.K.; Van der Eycken, E.V.; DePass, A.L.; et al. Synthesis and anti-inflammatory activity evaluation of novel chroman derivatives. *New J. Chem.* **2020**, *44*, 13716–13727.

37. Mohsin, N.u.A.; Irfan, M.; Hassan, S.u.; Saleem, U. Current Strategies in Development of New Chromone Derivatives with Diversified Pharmacological Activities: A Review. *Pharm. Chem. J.* **2020**, *54*, 241–257. [CrossRef]

38. Nalla, V.; Shaikh, A.; Bapat, S.; Vyas, R.; Karthikeyan, M.; Yogeeswari, P.; Sriram, D.; Muthukrishnan, M. Identification of potent chromone embedded [1,2,3]-triazoles as novel anti-tubercular agents. *R. Soc. Open Sci.* **2018**, *5*, 171750. [CrossRef]

39. Wang, G.; Chen, M.; Qiu, J.; Xie, Z.; Cao, A. Synthesis, in vitro α-glucosidase inhibitory activity and docking studies of novel chromone-isatin derivatives. *Bioorganic Med. Chem. Lett.* **2018**, *8*, 113–116. [CrossRef]

40. Sugiyama, T.; Narukawa, Y.; Shibata, S.; Masui, R.; Kiuchi, F. New 2-(2-Phenylethyl)chromone Derivatives and Inhibitors of Phosphodiesterase (PDE) 3A from Agarwood. *Nat. Prod. Commun.* **2016**, *11*, 795–797. [CrossRef]

41. Rao, Y.J.; Abhijit, K. Synthesis of Novel Functionalized Pyrano Annulated/Oxazolone Pendent Chromone Derivatives as Potent Anti-Diabetic Agents. *Russ. J. Gen. Chem.* **2020**, *90*, 1074–1082. [CrossRef]

42. Ivasiv, V.; Albertini, C.; Gonçalves, A.E.; Rossi, M.; Bolognesi, M.L. Molecular hybridization as a tool for designing multitarget drug candidates for complex diseases. *Curr. Top. Med. Chem.* **2019**, *19*, 1694–1711. [CrossRef] [PubMed]

43. Khilya, V.P.; Grishko, L.G.; Sokolova, T.N. Chemistry of heteroanalogs of isoflavones. III. Synthesis of benzimidazole and benzothiazole analogs of isoflavones. *Chem. Heterocycl. Compd.* **1975**, *11*, 1353–1355. [CrossRef]

44. Gorbulenko, N.V.; Frasinyuk, M.S.; Khilya, V.P. Chemistry of heteroanalogs of isoflavones. 16. Benzthiazole analogs of isoflavones. *Chem. Heterocycl. Compd.* **1994**, *30*, 405–412. [CrossRef]

45. Frasinyuk, M.S.; Turov, A.V.; Khilya, V.P. Chemistry of the hetero analogs of isoflavones. 22. Mannich reaction in the benzimidazole and benzothiazole analogs of isoflavones. *Chem. Heterocycl. Compd.* **1998**, *34*, 923–928. [CrossRef]

46. Andrews, S.P.; Mason, J.S.; Hurrell, E.; Congreve, M. Structure-based drug design of chromone antagonists of the adenosine A$_{2A}$ receptor. *MedChemComm* **2014**, *5*, 571–575. [CrossRef]

47. Frasinyuk, M.S.; Bondarenko, S.P.; Gorbulenko, N.V.; Turov, A.V.; Khilya, V.P. Cyclic Carboxylic Anhydrides as New Reagents for Formation of Chromone Ring. *J. Heterocycl. Chem.* **2014**, *51*, 768–774. [CrossRef]

48. Mrug, G.P.; Bondarenko, S.P.; Khilya, V.P.; Frasinyuk, M.S. Synthesis and aminomethylation of 7-hydroxy-5-methoxyisoflavones. *Chem. Nat. Compd.* **2013**, *49*, 235–241. [CrossRef]

49. Khilya, O.V.; Frasinyuk, M.S.; Turov, A.V.; Khilya, V.P. Chemistry of 3-Hetarylcoumarins. 1. 3-(2-Benzazolyl)coumarins. *Chem. Heterocycl. Compd.* **2001**, *37*, 1029–1037. [CrossRef]

50. Khilya, O.V.; Shablykina, O.V.; Frasinyuk, M.S.; Turov, A.V.; Ishchenko, V.V.; Khilya, V.P. Chemistry of 3-hetarylcoumarins. 2. 3-(2-thiazolyl)coumarins. *Chem. Heterocycl. Compd.* **2004**, *40*, 1408–1420. [CrossRef]

51. Katoueezadeh, M.; Pilehvari, N.; Fatemi, A.; Hassanshahi, G.; Torabizadeh, S.A. Inhibition of DNA damage response pathway using combination of DDR pathway inhibitors and radiation in treatment of acute lymphoblastic leukemia cells. *Future Oncol.* **2021**, *17*, 2803–2816. [CrossRef] [PubMed]

52. Meng, X.Y.; Zhang, H.X.; Mezei, M.; Cui, M. Molecular docking: A powerful approach for structure-based drug discovery. *Curr. Comput.-Aided Drug Des.* **2011**, *7*, 146–157. [CrossRef] [PubMed]

53. Mosmann, T. Rapid colorimetric assay for cellular growth and survival: Application to proliferation and cytotoxicity assays. *J. Immunol. Methods* **1983**, *65*, 55–63. [CrossRef]

54. van Meerloo, J.; Kaspers, G.J.; Cloos, J. Cell sensitivity assays: The MTT assay. *Methods Mol. Biol.* **2011**, *731*, 237–245. [PubMed]

55. Shaik, A.; Bhakuni, R.; Kirubakaran, S. Design, Synthesis, and Docking Studies of New Torin2 Analogs as Potential ATR/mTOR Kinase Inhibitors. *Molecules* **2018**, *23*, 992. [CrossRef] [PubMed]

56. Friesner, R.A.; Murphy, R.B.; Repasky, M.P.; Frye, L.L.; Greenwood, J.R.; Halgren, T.A.; Sanschagrin, P.C.; Mainz, D.T. Extra Precision Glide: Docking and Scoring Incorporating a Model of Hydrophobic Enclosure for Protein-Ligand Complexes. *J. Med. Chem.* **2006**, *49*, 6177–6196. [CrossRef]

57. Sastry, G.M.; Adzhigirey, M.; Day, T.; Annabhimoju, R.; Sherman, W. Protein and ligand preparation: Parameters, protocols, and influence on virtual screening enrichments. *J. Comput.-Aided Mol. Des.* **2013**, *27*, 221–234. [CrossRef]

58. Greenwood, J.R.; Calkins, D.; Sullivan, A.P.; Shelley, J.C. Towards the comprehensive, rapid, and accurate prediction of the favorable tautomeric states of drug-like molecules in aqueous solution. *J. Comput.-Aided Mol. Des.* **2010**, *24*, 591–604. [CrossRef]

59. Shelley, J.C.; Cholleti, A.; Frye, L.; Greenwood, J.R.; Timlin, M.R.; Uchimaya, M. Epik: A software program for pKa prediction and protonation state generation for drug-like molecules. *J. Comput.-Aided Mol. Des.* **2007**, *21*, 681–691. [CrossRef]